Organic Process Research & Development

Article

pubs.acs.org/OPRD

Rapid Development and Scale-Up of a 1*H*-4-Substituted Imidazole Intermediate Enabled by Chemistry in Continuous Plug Flow Reactors

Scott A. May,* Martin D. Johnson,* Timothy M. Braden, Joel R. Calvin, Brian D. Haeberle, Amy R. Jines, Richard D. Miller, Edward F. Plocharczyk,‡ Gregory A. Rener, Rachel N. Richey, Christopher R. Schmid, Radhe K. Vaid, and Hannah Yu

Chemical Product Research and Development, Eli Lilly and Company, Indianapolis, Indiana 46285, United States

Supporting Information

ABSTRACT: The development of reactions in a continuous fashion in plug flow tube reactors (PFR) offers unique advantages to the drug development and scale-up process and can also enable chemistry that would be difficult to perform via batch processing. Herein, we report the development of two different continuous flow approaches to a key 1*H*-4-substituted imidazole intermediate (**5**). In a first generation approach, rapid optimization and scale-up of a challenging cyclization reaction was demonstrated in a PFR under GMP conditions to afford 29 kg of protected product **2**. This material was further processed in batch equipment to deliver di-HCl salt **4**. This first generation approach highlights the rapid development of chemistry in research-scale PFRs and speed to material delivery through linear scale up to a pilot-scale PFR under GMP conditions. In a second generation effort, a more efficient synthetic route was developed, and PFRs with automated sampling, dilution, and analytical analysis allowed for rapid and data-rich reaction optimization of both a key cyclization reaction and thermal removal of a Boc protecting group. This work culminated in 1 kg demonstration runs in a 0.22 L PFR for both continuous steps and shows the potential of commercialization from a lab hood footprint (1−2 MT/year).

INTRODUCTION

The synthesis of nitrogen-containing heterocycles has long been a topic of intense research.[1,2] This is due, in large part, to the importance of these compounds as drug candidates. The vast majority of new molecular entities (NMEs) contain at least one nitrogen atom in the chemical structure. A subcategory of these compounds are imidazoles, which are notable pharmacophores in a number of areas of discovery chemistry research.[3,4] Appropriately, numerous synthetic approaches to these compounds have been published in the literature.[5] We required a robust synthetic route toward 1*H*-4-substituted imidazole **5** (Scheme 1), and the existing synthetic approaches to these ring systems, while well documented, resulted in poor isolated yields of **2** due to the tendency towards starting material (**1**) oligomerization under the reaction conditions. Lower temperature regimes (room temperature →70 °C) favored oligomerization, while at higher temperatures (>100 °C), cyclization was favored. Lower yield would be anticipated with increased scale due to less efficient heat transfer as the batch reactor size increases. To enable rapid scale-up of this reaction for an early phase delivery, an approach involving a plug flow reactor (PFR) was used. The high surface area-to-volume ratio afforded by the PFR allowed for rapid heat-up to a productive temperature regime with the ability to maintain constant time to reaction temperature with scale-up. This allowed the key imidazole cyclization to scale linearly from 1.75-mL research-scale reactors to a 7.1-L pilot-scale reactor. Additionally, the ability to run at high pressure in a tubular reactor allowed for the use of a lower-boiling solvent (MeOH) that greatly simplified the isolation of **2**. This process afforded 29 kg of **2** after batch isolation. Imidazole **2** was then transformed in two steps to amine **5** via alkylation, protecting group removal, and neutralization (Scheme 1).

In a second generation approach to **5**, the synthetic strategy was significantly altered to address processing concerns, and *N*-methyl ketoamide **6** was used as the starting point (Scheme 2). PFRs were utilized in both the cyclization of **6** to afford imidazole **3** and in a thermal protecting group removal to afford free amine **5**. This effort also utilized automated sampling and dilution allowing for data-rich experimentation, fast reaction optimization and scale up. Herein we describe the development and continuous processing technology used in both first- and second generation routes to 1*H*-4-substituted imidazole intermediate **5**.

RESULTS AND DISCUSSION

First Generation Approach to Ketoamide 1. The initial small-scale approach to ketoamide **1** was first developed for the desfluoro analogue **11** (Scheme 3). Direct displacement of phenacyl bromide **7**[6] with hexamethylenetetramine (HMTA) in chlorinated solvents led to the corresponding amine salt **8**, which was isolated by filtration. Hydrolysis under aqueous acidic conditions led to low and unreproducible yields of phenacyl amine hydrochloride salt **9**. Phenacyl amine **9** was found to be contaminated with residual ammonium chloride, which could not be easily removed. This, in turn, complicated the coupling reactions between **9** and *N*-Boc-isonipicotic acid (**10**) and led to mixtures of the primary amide of

Special Issue: Continuous Processes 2012

Received: December 3, 2011
Published: April 19, 2012

   dx.doi.org/10.1021/op200351g | *Org. Process Res. Dev.* 2012, 16, 982−1002

Scheme 1. First generation approach to *N*-methyl imidazole 5

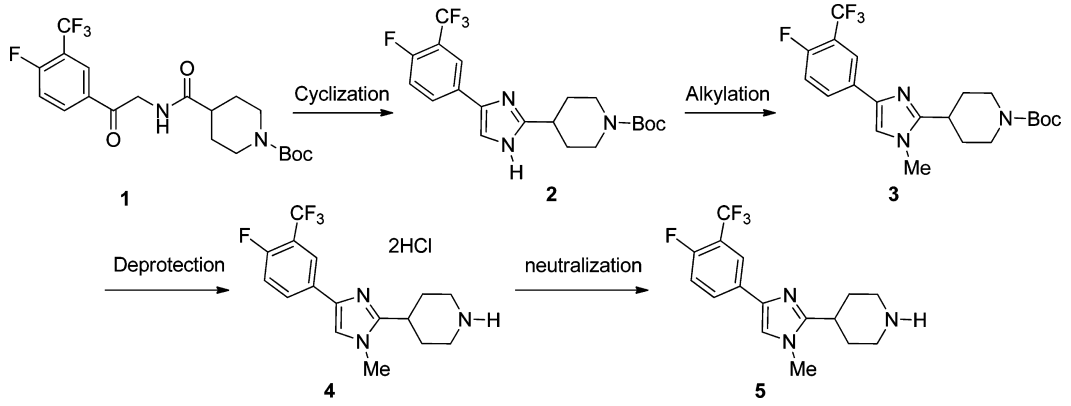

Scheme 2. Second generation approach to *N*-methyl imidazole 5

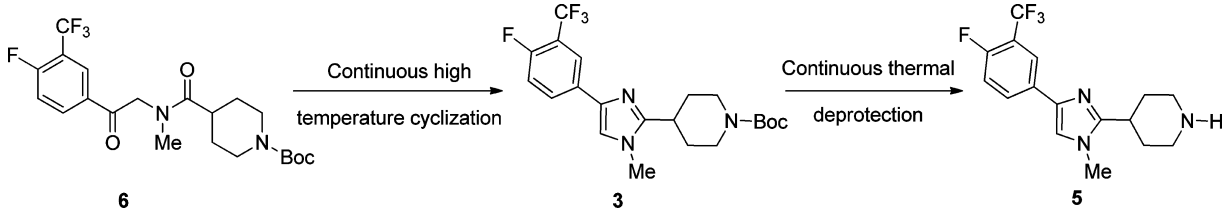

Scheme 3. Initial synthesis of imidazole 13 via des-fluoro ketoamide 11

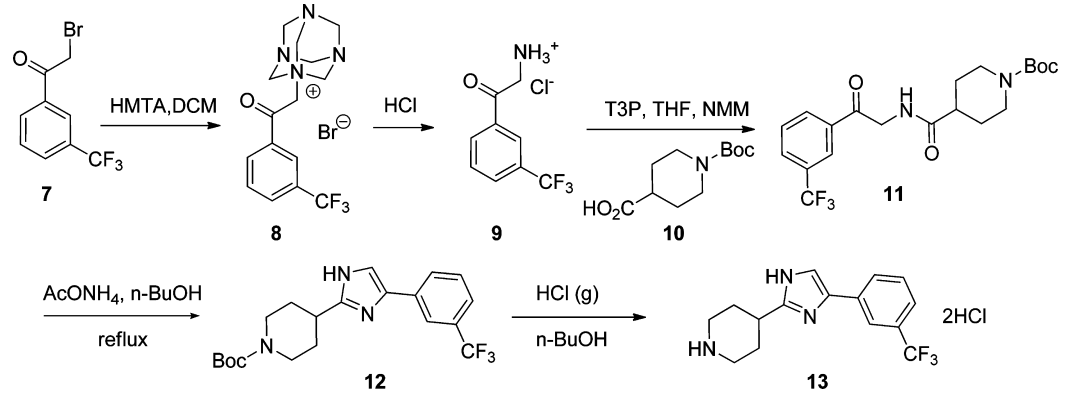

Scheme 4. Synthesis of ketoamide 11 via azide/Staudinger sequence

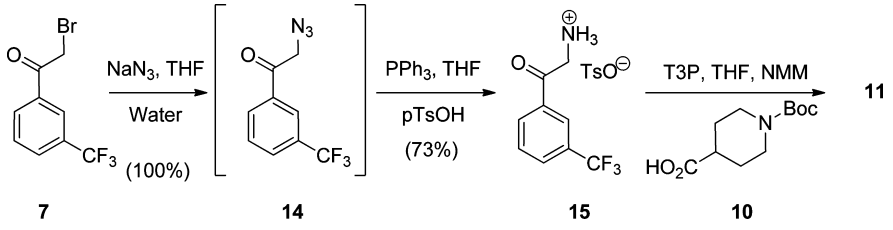

10 along with the desired product (**11**), which were also difficult to purify. The synthesis of **12** was then completed by thermal cyclization with ammonium acetate in 1-butanol, which afforded 1H-imidazole **12**. Treatment of the imidazole product directly with gaseous HCl delivered the amine salt **13** in good yield and purity.

By building off of the general approach shown in Scheme 3, an alternative route was developed to tosylate salt **15**, which had excellent physical properties and could be obtained in high yield and purity (Scheme 4). The displacement of phenacyl bromide **7** with sodium azide in water-wet tetrahydrofuran[7] afforded azide **14** which was telescoped directly into a Staudinger reduction.[8] Using 1.05 equiv of triphenylphosphine in THF in the presence of 1.0 equiv of *p*-toluenesulfonic acid monohydrate the crude azide (**14**) was efficiently reduced, and the corresponding tosylate salt **15** crystallized directly from solution in good yield and in excellent purity. The amide coupling reaction with 2-propanephosphonic acid anhydride (T3P) afforded ketoamide **11** in high yield and purity (Table 1).

The chemistry in Scheme 4 was then scaled up and also applied to desired ketoamide analogue **1** (Table 1). On 22 L scale the process performed well as the amine salts **15a** and **15b** were all isolated in good yield and purity. The coupling reaction

dx.doi.org/10.1021/op200351g | *Org. Process Res. Dev.* 2012, 16, 982–1002

Table 1. Scale-up results for the synthesis of ketoamides 11 and 1

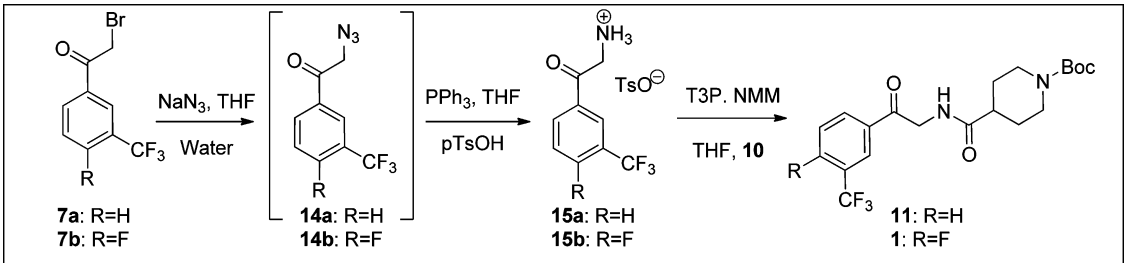

entry	kg **7**	yield **15** (purity)	kg **15**	yield **11** or **1** (purity)
1: R=H	1.65 kg	73% (100%)	0.74 kg	**11**: 81% (>99%)
2: R=F	1.00 kg	92% (99.9%)	1.1 kg	**1:** 90% (99.9%)
3: R=F	78.5 kg	90% (99.7%)	58 kg	**1**:73%* (99.5%)

*Conditions: CDI, EtOAc/THF.

Scheme 5. Small-scale batch synthesis of imidazole 13

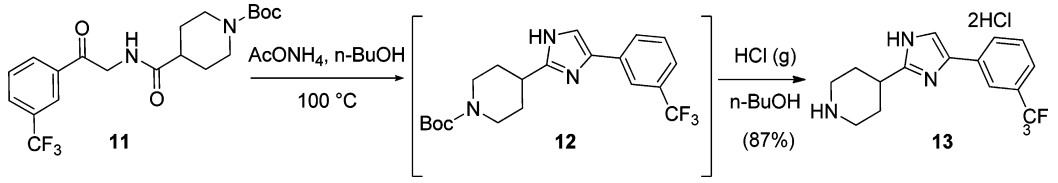

between **15** and *N*-Boc-isonipecotic acid (**10**) performed well using T3P in THF containing *N*-methylmorpholine. However, due to difficulty sourcing T3P on scale, the conversion of **15b** to **1** was accomplished with carbonyl diimidazole in a mixture of ethyl acetate and THF (entry 3). This process afforded comparably pure product, but with lower overall yield.

Development of a First Generation Cyclization Reaction. The initial small scale cyclization reactions with ketoamide **1** were once again based on encouraging results from the desfluoro compound **11** (Scheme 5). Cyclization in butanol in a sealed tube[9] allowed for complete conversion (**11**→**12**) in 24 h. The reaction optimization and workup was straightforward and amine salt **13** was obtained in 87% yield upon treatment with gaseous HCl in n-butanol. However, the cyclization reaction slowed markedly in a scale up attempt in traditional glassware due to loss of ammonia from the reaction at elevated temperature. This reaction required multiple charges of ammonium acetate and, ultimately, resubmission of the crude product to the reaction conditions to achieve full conversion.

In order to scale this chemistry to kilogram quantities we sought a more efficient process and turned to a PFR approach where the cyclization reaction could be conducted at high temperature and pressure in methanol (Figure 1). Continuous reactions in this paper required temperatures in the range 100−270 °C, pressures up to 70 bar, and mean residence time (τ) in the range 5−90 min. Tubular reactors were constructed from 316 L seamless stainless steel which provided good corrosion resistance with high pressure and temperature ratings at low cost. Nine PFRs with volumes from 1.75 to 7140 mL were used in the chemistry described in this paper. All nine PFRs used in this study have been characterized (Table 10) on the basis of axial dispersion number (D/uL), pressure drop, and heat transfer surface area per unit volume (A/V). It is important to recognize that actual mean residence time (τ) and calculated mean

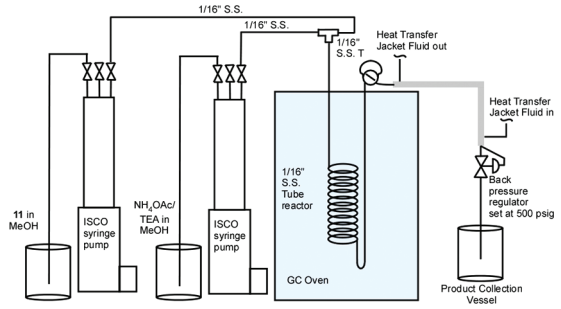

Figure 1. Continuous thermal tube reactor setup for reaction optimization.[13]

residence time based on reactor volume and feed flow rates are typically different. In a later section we will show an example where τ differs by as much as 40% because of density and phase changes at higher temperatures. In this paper we refer to mean residence time (τ) only when measured on the basis of F-curve output, which is described in a later section of this paper. In the absence of a measured residence time (τ) we report this value as total reactor volume ($V_{reactor}$) divided by the total volumetric flow rate (Q_{feed}).

Methanol was chosen as solvent since it allowed for homogeneous solution feeds of ammonium acetate and ketoamide **11** at room temperature. The crude product (**12**) was also soluble in methanol at room temperature which minimized the risk of reactor fouling. High pressure syringe pumps fed starting materials through stainless steel tubing with 1.59 mm outside diameter (o.d.) and 0.56 mm inside diameter (d) into a 1.75 mL PFR[10] with a $V_{reactor}/Q_{feed}$ = 45 min.[11] The PFR was heated in a programmable GC oven which allowed for rapid temperature screening or a temperature program if desired.[12] The product solution exited the GC oven, passed through a heat exchanger, through a back pressure regulator and arrived at a product

dx.doi.org/10.1021/op200351g | Org. Process Res. Dev. 2012, 16, 982−1002

collection vessel which was at room temperature and atmospheric pressure.

Seven different conditions were evaluated[14] for the cyclization of ketoamide **11** in a single day (Figure 2). In the case of ketoamide **11**, loss of the Boc group was not a concern since the next step was protecting group removal and the deprotected product (**13**) could be extracted into an organic phase along with the desired product **12** during workup. Full conversion was accomplished with $V_{reactor}/Q_{feed}$ = 45 min at 170 °C.[15] This initial temperature screen was followed by a stoichiometry screen in the same equipment set, but without triethylamine.[16] Ammonium acetate (1, 5, and 10 equiv) was examined at 170 °C and 5 equiv was selected as optimal for this temperature and residence time (<2% **11**; >95% products). Once again the entire range of experiments was conducted in a single working day[17] using just 5 g of ketoamide **11**.[18]

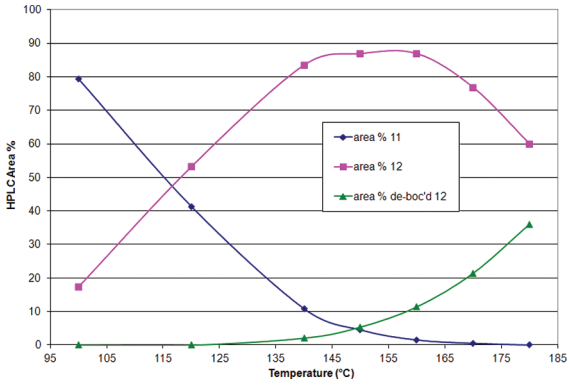

Figure 2. Temperature screening for the cyclization of **11** in a PFR with $V_{reactor}/Q_{feed}$ = 45 min.

The cyclization and deprotection sequence was scaled up to 20 g then to 775 g[19] using the general equipment setup shown in Figure 1, the exception being differences in reactor dimensions (Table 2). Accordingly, the 26× scale-up in reactor volume and flow rate from Table 2, entries 1 and 2, resulted in almost identical results. If the process shown in Table 2, entry 2, were run continuously (24/7), the 541 mL reactor in a GC oven in a laboratory hood could process 4.6 kg/day or 32.5 kg/week of ketoamide **11**. One can easily see that, even with modest scale-up beyond this reactor size, very high throughput could be obtained even in a standard laboratory hood. This reaction was scaled up successfully in three different PFRs based on $V_{reactor}/Q_{feed}$ data and not τ. This was possible because the same thermal expansion of the single liquid phase and reactor characteristics (same heat-up time, negligible axial dispersion, and negligible temperature gradients after heat-up) were maintained in each PFR.

With the impressive results from ketoamide **11** (Table 2), we sought to apply these conditions to ketoamide **1**, which contained an additional fluorine atom on the aromatic ring. In addition, we required the differentially protected product **2** (which demanded a more finely tuned set of reaction conditions) to maximize desired product while minimizing deprotected amine **16** (Scheme 6). This small variation in structure proved quite impactful, however, as initial batch cyclization conditions afforded much lower yields (50−60%) of product **2**. In addition to the desired imidazole **2** and deprotected product **16**, significant formations of aniline analogue **17** and dimer **18** were observed.[20]

The first efforts to obtain larger quantities of **2** involved batch reactions in 2 L glass pressure vessels with *n*-butanol as solvent at 100 °C.[21] The cyclization reaction was performed four times (200−250 g scale each), and the crude product solutions were combined. A single, labor-intensive workup and isolation afforded ∼500 g of **2** in 56% yield. In contrast to substrate **11**, the reaction with **1** became orange upon stirring at elevated temperature, and sticky yellow solids formed during isolation attempts. Fortunately, trituration of the crude product

Table 2. PFR cyclization results for ketoamide (11) cyclization and deprotection

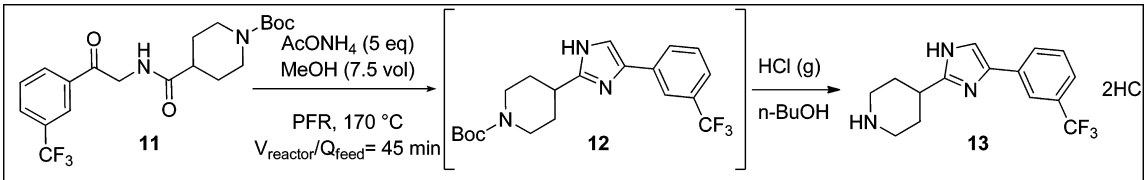

entry	scale (g)	run time (h)	reactor volume (mL)	flow rate mL/min	% yield (% purity)
1	20	7.5	20.5	0.456	90 (99.9)
2	775	4	541	12.02	92 (99.5)

Scheme 6. Cyclization of ketoamide 1 with known processing impurities

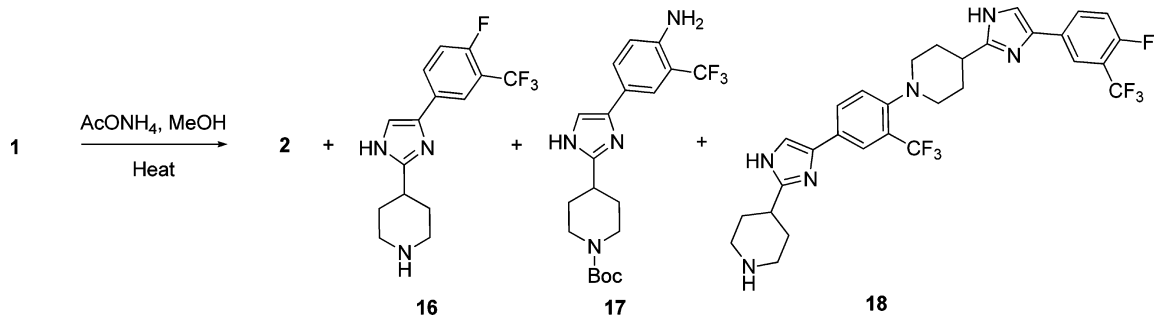

dx.doi.org/10.1021/op200351g | Org. Process Res. Dev. 2012, 16, 982−1002

with acetonitrile resulted in clean, off-white solids with very good handling properties and impurity profile.

A closer examination of several batch scale-up results (Figure 3) revealed that reaction performance was declining as reaction scale

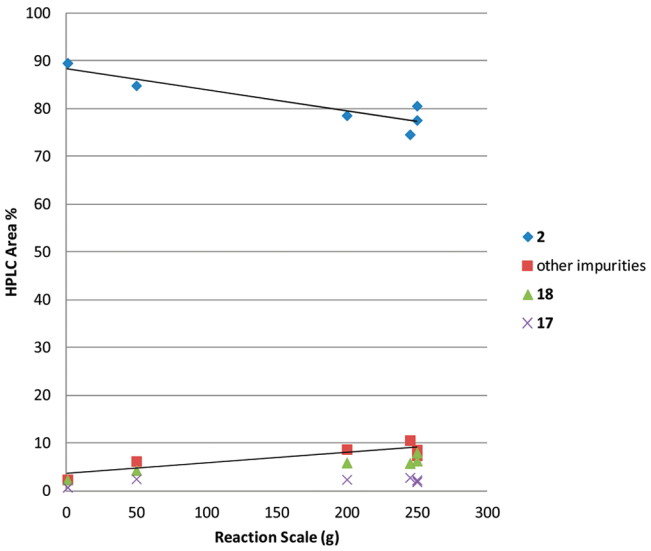

Figure 3. Trends in the batch cyclization of ketoamide **1**.

increased. For example, area % of product **2** at 250-g scale was 10% lower than at the initial 1-g scale reaction. This drop in product area % was mirrored by an increase in other impurities as well. Since heat-up times lengthen in batch reactors as scale increases, longer time periods in an unproductive thermal regime would be anticipated during scale-up. It appeared as though lower-temperature regimes (room temperature → 70 °C) favored greater degradation, while at higher temperatures (>70 °C) cyclization was favored.

With a 25 kg delivery of **2** looming, we determined that traditional batch scale up was not a viable option and we again chose to develop the cyclization of **1** in a PFR. We were confident that this would address any issues associated with heating rates and would also afford precise control of time at reaction temperature. We also suspected that we could improve the isolation of the product (**2**) by running in methanol, a solvent amenable to direct crystallization.

Probing temperature while holding constant $V_{reactor}/Q_{feed}$ at 90 min indicated that a temperature range of 140−150 °C was optimal at this reaction time with 5 equiv of ammonium acetate (Figure 4). Shorter calculated residence times suffered from incomplete conversion, and at higher temperatures extensive loss of the protecting group was observed.

Preferred conditions were 10 equiv of ammonium acetate in 3 vol equiv of methanol at 140 °C with $V_{reactor}/Q_{feed}$ = 90 min. Once optimal conditions were determined, a series of scale-up experiments (Table 3, entries 1−3) were conducted ahead of a

Table 3. Summary of cyclization of 1 using different plug flow reactor sizes

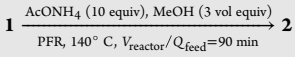

entry	reactor size (mL)	**2** (%)	**1** (%)	De-Boc **16** (%)	aniline **17** (%)	other impurities (%)
1	4.51	79.13	4.4	4.32	2.02	8.14
2	143	80.34	0.51	4.73	7.02	5.03
3	1462	81.75	1.32	3.35	6.6	3.82
4	7140	82.9	1.03	5.7	4.56	4.39

GMP run (entry 4) where 55 kg of ketoamide **1** was processed over 141 h at steady state in a 7.1 L PFR. The data in Table 3 represent average values at steady state. The consistency of reaction performance across this wide range of reactor sizes can be attributed to the fact that the reaction solution was a single homogeneous phase, thermal expansion was the same at all scales, axial dispersion was negligible for the coiled tube reactors at all scales from 4.51 to 7140 mL (Table 10), and the highest practical A/V was used at each scale to achieve essentially isothermal conditions.

While the product profile average from the GMP campaign looked very similar to the runs in smaller reactors (Table 3), close review of the profile as a function of time indicated a subtle, but steady linear decline in product area % (Figure 5). Likewise the dimer impurity (**18**) trended higher over time. These two observations in combination with the fact that the starting material feed solutions were prepared in advance and allowed to stand for the prolonged time of the 6-day continuous run suggested that the

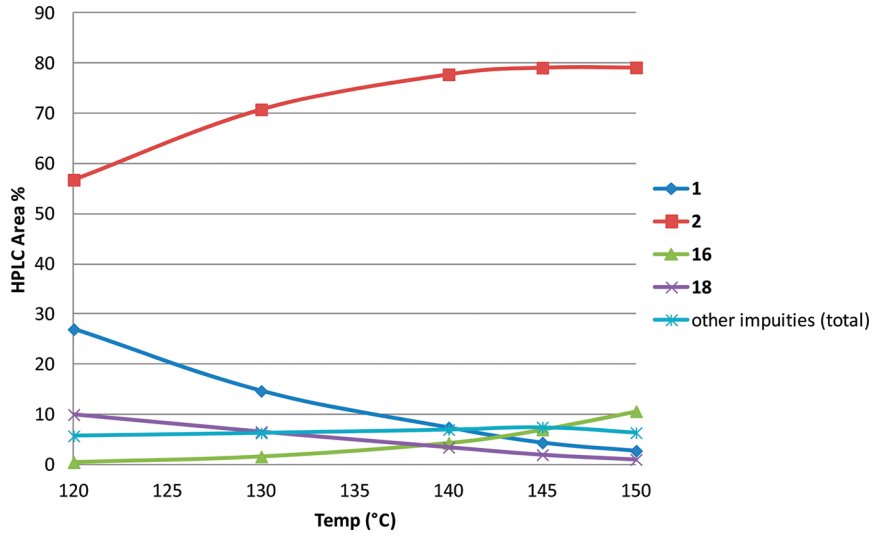

Figure 4. Temperature screen for the cyclization of **1**.[22]

dx.doi.org/10.1021/op200351g | Org. Process Res. Dev. 2012, 16, 982−1002

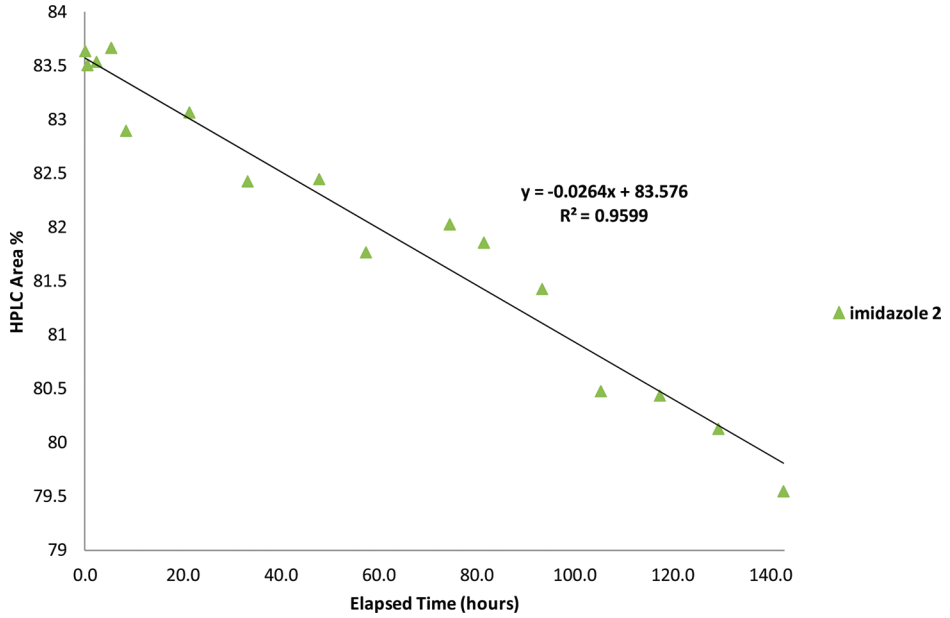

Figure 5. Product (**2**) area % trends in cyclization reaction in 7.1 L PFR.

ketoamide **1** was degrading over time in the presence of ammonium acetate even at room temperature.

We had conducted a brief stability study of **1** prior to the campaign but not of a duration close to the time needed to complete the campaign (141 h). In this study no noticeable degradation was observed by HPLC area % or ^{1}H NMR. Closer examination of ketoamide **1** stability by wt % indicated a startling degradation profile (Figure 6). What was even more surprising was that even at

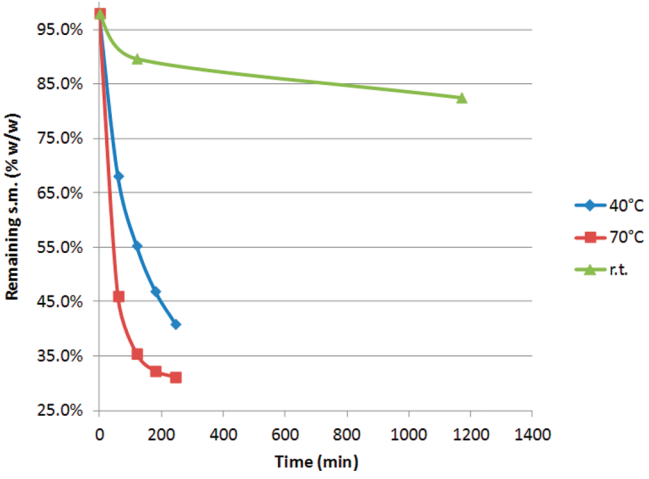

Figure 6. Stability of 1 in the presence of ammonium acetate.

room temperature the steady drop in ketoamide **1** weight % was observed with just a small change in HPLC area %. No significant product formation or deprotection was observed at room temperature to account for the loss in potency. The solutions at elevated temperature showed visible signs of degradation such as a dark-orange/red color. Clearly, separate feed streams of ketoamide and ammonium acetate would have been more appropriate. Subsequently, it is standard practice to test stability of all reagent feed solutions for the time durations that would be expected in a manufacturing facility.

On the basis of this stability study, it was clear that oligomerization pathways were operable. The observation of dimer **18** indicated that the aromatic ring was activated towards nucleophilic aromatic substitution under reaction conditions. A number of different degradation pathways were possible with various nitrogen nucleophiles as depicted in Scheme 7. However, it was also clear that the imidazole products were not susceptible to similar degradation pathways.[23] This is not surprising since the aryl fluoride would be much less activated toward S_NAr with the imidazole present and not the ketone.

The fact that long $V_{reactor}/Q_{feed}$ times at 140 °C were optimal for this reaction was interesting, given the rapid degradation observed in Figure 6 . One possible explanation for why conversion to product was favored at higher temperature was that activation energy for conversion to product may be higher than activation energies of the side reaction indicated by rate k_2 or k_3 (Scheme 8). The temperature dependence of a reaction rate constant can be quantified by the Arrhenius Law.[24] The larger the activation energy for a reaction, the more temperature sensitive the rate of reaction. This could cause the relative rates of conversion to product and decomposition of **1** to be more favorable toward the product **2** at higher temperatures.

Two sections of product (**2**) solution were produced from the 7.1-L PFR reaction under GMP standards, and each section was transferred to a pilot-scale batch reactor for workup and isolation.[25] The extraction, concentration, and addition of acetonitrile and water afforded a technical grade product with about 80% potency. The combined sections of crude imidazole product **2** were then reslurried in acetonitrile to afford 29.2 kg of purified imidazole in 52% isolated yield (potency corrected). Imidazole **2** was then regioselectively alkylated with methyl iodide using potassium hydroxide in DMSO to afford **3** in 90% isolated yield after crystallization (Scheme 9). The crude product was recrystallized from ethanol and water in 93% yield to remove aniline impurity **25** (Scheme 11). A total of 28.5 kg of **2** was processed through this sequence to give **3** in 82% isolated yield. Methyl iodide was controlled to <5 ppm in the product after recrystallization. Protecting group removal (**3**→**4**) was accomplished in methanol using anhydrous HCl (4 equiv) generated in situ from methanol and acetyl chloride at room temperature. Over 99% conversion was obtained in 13 h with no new observable impurities forming. Solvent exchange from methanol to DMSO followed by treatment

dx.doi.org/10.1021/op200351g | Org. Process Res. Dev. 2012, 16, 982–1002

Scheme 7. Possible S_NAr-based degradation pathways

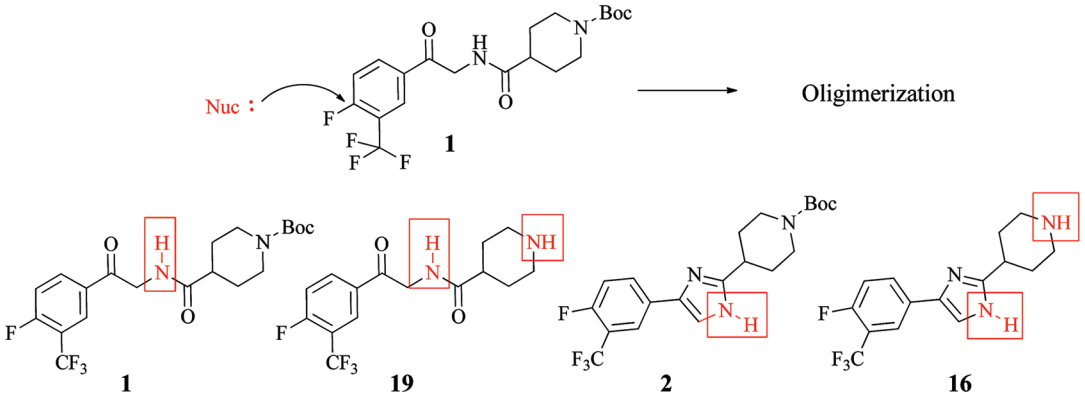

Scheme 8. Rationale for temperature-dependent degradation

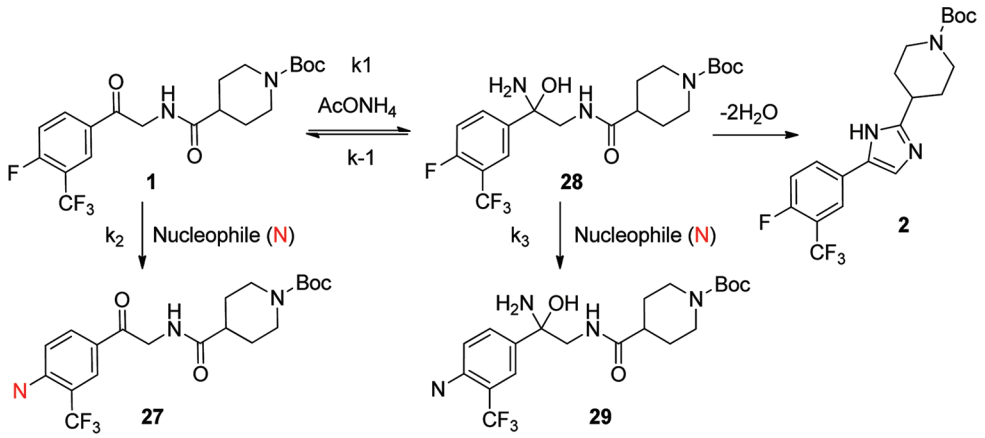

Scheme 9. Synthesis of 5 from imidazole 2

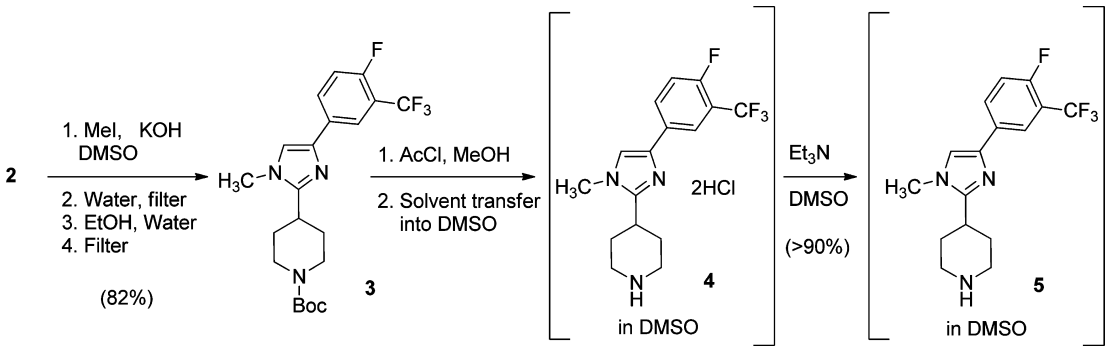

with triethylamine afforded free amine **3**, which was forward processed directly in high yield in chemistry that will not be discussed in this account.

While the overall sequence of this process was effective in delivering material at kilogram scale in serviceable yield, there were several undesirable aspects including the following:

(1) The cyclization yield was low and required reprocessing to afford material of acceptable quality.

(2) The use of methyl iodide, a compound that needed to be controlled at ppm levels in **3**.

(3) Aniline byproduct **18** must be rejected to low (ppm) levels in intermediate **3**.

(4) Removal of the Boc protecting group and salt break, while high yielding, were inefficient and wasteful processes. The use of 4 equiv of HCl was also not ideal.

(5) The synthesis of ketoamide **1** involved the use of bromide **7b** (a strong lachrymator), azide (safety hazard), and a Staudinger reaction which generates triphenylphosphine oxide and nitrogen during the reaction.

Second Generation Approach using *N*-Methyl Ketoamide 6. To address aspects 1 and 2 we sought a simple structural change from ketoamide **1** to *N*-methyl ketoamide **6**. On the basis of the degradation pathways suggested in Scheme 7 blocking the amide nitrogen would eliminate the primary degradation pathway and allow for a much higher yield of product. Regarding point 4, we had already observed thermal cleavage of the Boc group under the cyclization conditions at high temperatures. We wanted to further exploit the benefits of the PFR and develop an efficient thermal protecting group removal

dx.doi.org/10.1021/op200351g | *Org. Process Res. Dev.* 2012, 16, 982–1002

Scheme 10. Synthesis of *N*-methyl ketoamide 6 from *N*-Boc sarcosine (20)

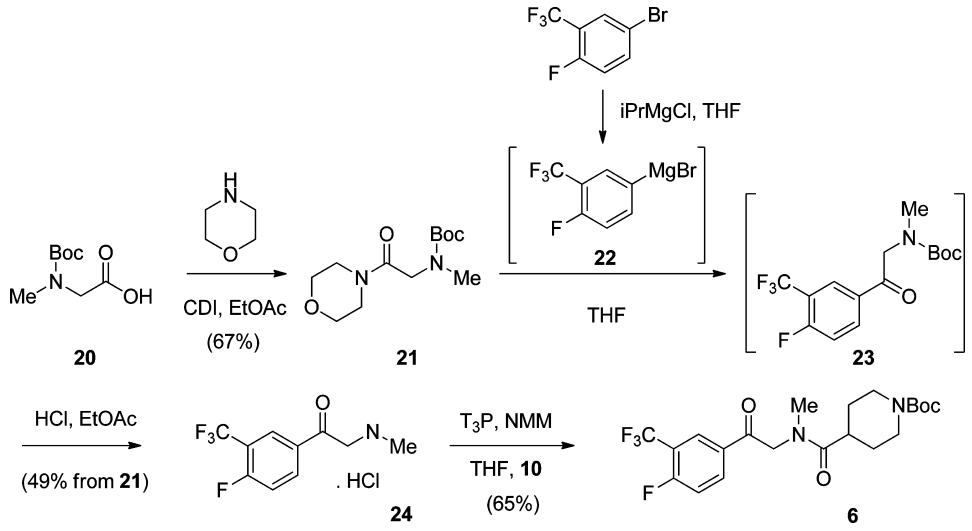

Scheme 11. Cyclization of ketoamide 6

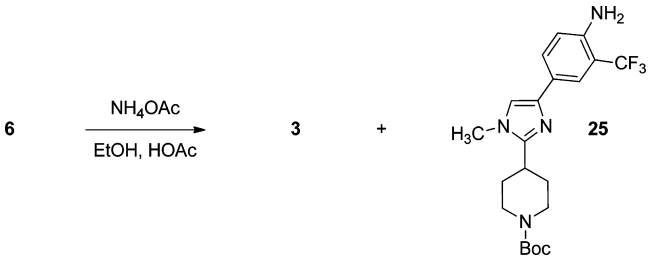

to eliminate any reagents in the reaction. Finally, we sought a redesigned route to *N*-methyl ketoamide **6** to eliminate the undesirable reagents and unit operations in the current ketoamide synthetic route (Table 1).

The synthetic route to *N*-methyl ketoamide **6** (Scheme 10) was designed from *N*-Boc-protected sarcosine (**20**), a readily available starting material that has the required methyl group "pre-installed" avoiding any type of downstream alkylation. *N*-Boc sarcosine (**20**) was converted to the morpholine amide **21** using standard conditions in modest yield. The crude amide **20** was treated directly with Grignard reagent (**22**)[26] to afford aminoketone **23**. Treatment of **23** with HCl(g) in ethyl acetate resulted in the salt of *N*-methylphenacylamine (**24**). The synthesis was completed through an amide coupling between **24** and **10** with T3P in THF in 69% isolated yield. This unoptimized process was used to synthesize 2 kg of *N*-methyl ketoamide **6** which funded scale-up studies in flow.

Development of a Second Generation Cyclization Reaction from Ketoamide 6. Prior to PFR work on ketoamide **6**, it was found that adding acetic acid[27] (10 equiv with respect to starting ketoamide) to the cyclization conditions reduced the formation of aniline **25** (Scheme 11). Ketoamide **6** also cyclized to **3** at a much faster rate than ketoamide **1** cyclized to **2**. The faster rate of cyclization with *N*-methyl ketoamide **6** can be attributed to steric interactions which place the amide in a more favorable conformation for cyclization. The faster rate of cyclization also affects the rate of aniline analogue **25** formation. For example, treatment of ketoamide **6** with ammonium acetate (10 equiv) in methanol (sealed tube) at 104 °C resulted in full conversion in just 4 h. The amount of aniline analog **25** produced during the reaction was 0.61% area by HPLC. The isolation of this small-scale reaction afforded 80% of desired product **3** with aniline levels dropping by about half to 0.35%. When acetic acid (20 equiv) was added to a similar cyclization reaction in ethanol at 80 °C with 10 equiv of ammonium acetate, just 0.2% aniline could be detected by HPLC after 18 h. The product (**3**) was obtained in 91% yield, and aniline levels were determined to be 29 ppm in the isolated solid after crystallization. Overall, use of the *N*-methyl substrate **6** (over ketoamide **1**) cut aniline formation by about 10× (6% → 0.6%) and adding acetic acid to the cyclization of **6** dropped aniline formation another 3× (0.6% → 0.2%).

Given the issues with ketoamide **1** in the presence of ammonium acetate at room temperature, a stability study was performed with ketoamide **6**. We were pleased to find that *N*-methyl ketoamide **6** began to cyclize at room temperature in the presence of ammonium acetate. Additionally, formation of cyclized product **3** tracked almost identically with wt % drop in ketoamide **6**. This supported the hypothesis that S_NAr of the amide nitrogen was the primary degradation pathway (Scheme 7).

While the new batch cyclization conditions in ethanol with acetic acid were impressive this reaction suffered from two problems. First, long reaction times (16−20 h) were required to reach completion. Second, much like previous examples, the best results were those conducted in sealed tubes to prevent loss of ammonia. In addition, ammonium salts are known to sublime which may result in resolidification on colder surfaces in a batch tank. The possibility of process piping in the reactor head (including the reactor safety pressure relief) becoming blocked by solid ammonium acetate seemed real.[28,29] Addressing these two problems was the initial goal of developing a continuous flow process for this cyclization.

Initial cyclization PFR screening was conducted in a mixed ethanol/methanol solvent system. Methanol was added to improve solubility of ammonium acetate.[30] Two feed solutions were used: the first contained **6** in ethanol (3 mL/g), the second contained ammonium acetate (10 equiv) and acetic acid (20 equiv) in a mixture of EtOH (3 mL/g of **6**) and MeOH (1.5 mL/g of **6**). With stable feed solutions in hand, we chose $V_{reactor}/Q_{feed}$ = 15 min as a starting point and temperatures from 100 to 190 °C were screened in 10 °C intervals. At temperatures up to 130 °C, some starting material remained, but the reaction was otherwise clean by HPLC. However, the cyclized

dx.doi.org/10.1021/op200351g | *Org. Process Res. Dev.* 2012, 16, 982−1002

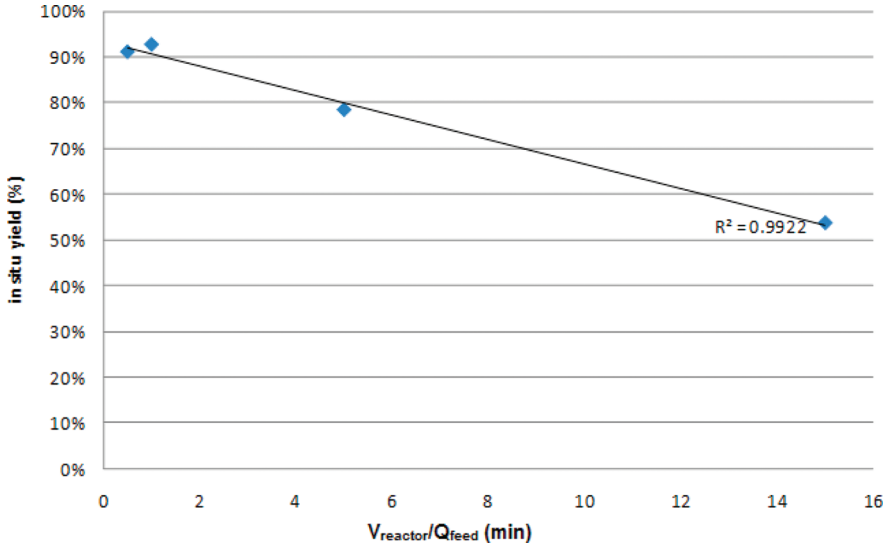

Figure 7. Effect of residence time on yield (wt%) of **3** at 190 °C: thermal deprotection.

product **3** underwent thermal deprotection at a rate that increased linearly as residence time increased at 190 °C (Figure 7).

Since the next step in the process was deprotection, we considered the possibility of performing both cyclization and deprotection reactions in the same PFR as a single telescoped process. Unfortunately, at temperatures above 170 °C a new, acylated impurity (**26**) began to form (Figure 8). In addition,

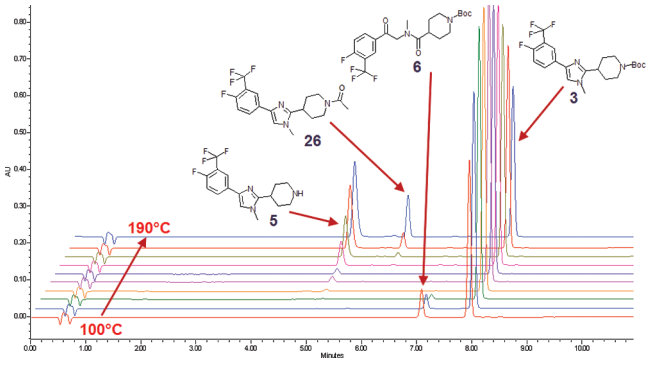

Figure 8. HPLC traces for cyclization temperature screen at $V_{reactor}/Q_{feed}$ = 15 min: 100 to 190 °C.

crystallization of **3** at this stage was the most efficient control point for aniline impurity **25**. For these reasons the cyclization and thermal deprotection were developed as separate chemical steps.

A residence time and temperature study for the cyclization of 6 was conducted at $V_{reactor}/Q_{feed}$ ranges from 1 to 60 min and a temperature range from 100 to 190 °C (Figure 9). In general, temperatures <110 °C suffered from low in situ yields due to incomplete conversion. Higher temperatures in the cyclization led to more deprotection but when the amounts of product, starting keto-amide and deprotected product were summed, nearly all of the mass could be accounted for, indicating that the polymerization was minimal. Optimal conditions of 140 °C and $V_{reactor}/Q_{feed}$ = 15 min were selected which maximized conversion while minimizing thermal deprotection.[31] Under these conditions the reaction was 80 times faster than the batch reaction conditions and could potentially deliver production-scale quantities in small PFR.[32]

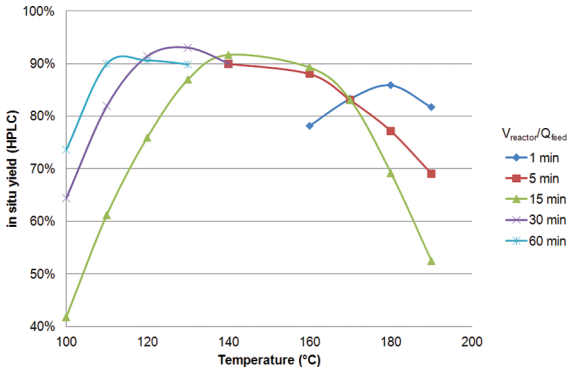

Figure 9. Cyclization in situ yield of **3** with respect to $V_{reactor}/Q_{feed}$ and temperature.

Isolation of crystalline **3** was accomplished by addition of water as antisolvent to the reaction mixture. Later work showed that comparable results were obtained with methanol as the sole solvent, which simplified the reaction. The reaction rate was slightly faster in methanol and the product could still be crystallized directly by addition of water. The aniline impurity (**25**) level in the isolated product from direct crystallization (unoptimized) from methanol and water was <50 ppm. These results were comparable to the batch process which provided **3** with 29 ppm of **25** under optimized conditions.

This process was successfully scaled up in a 221 mL PFR with 1232 g of *N*-methyl ketoamide **6**. The reaction was conducted at 140 °C with a τ = 10.7 min. This provided **3** in 80% isolated yield (88% in situ). A comparison of the batch and flow processes for the cyclization is summarized in Table 4.

Development of a Thermal Boc Group Deprotection Reaction. The next task was to develop a PFR process that could take advantage of the thermal Boc deprotection observed previously in the cyclization reaction screening (Figure 9). The *N*-Boc-protected imidazole **3** was dissolved in MeOH (7 mL/g), and a temperature screen was conducted at $V_{reactor}/Q_{feed}$ = 30 min. The desired thermal deprotection proceeded but a new, unidentified impurity arose at temperatures >180 °C (Figure 10). While the new impurity was not isolated and identified, it seemed possible that it was the result of reaction of **3** with MeOH since reactions in THF led to extremely

dx.doi.org/10.1021/op200351g | *Org. Process Res. Dev.* 2012, 16, 982–1002

Table 4. Comparison of batch and flow processes for N−H cyclization

process	solvent	volumes	temp (°C)	time	isolation	**25** (ppm)	yield (%)
batch	EtOH/HOAc	6	80	13−20 h	water addition	30	85
PFR	MeOH/HOAc	6.5	140	10 min	water addition	48	80[33]

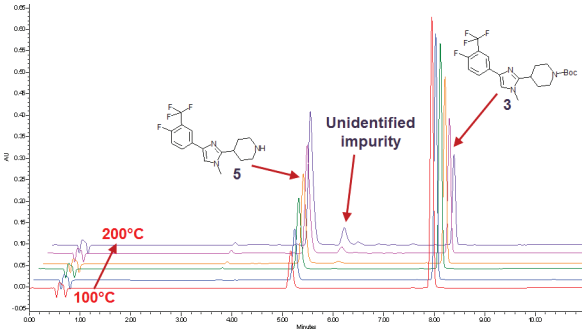

Figure 10. Thermal deprotection in MeOH, HPLC profiles.

clean profiles. However, THF resulted in a slower reaction rate than in methanol (~5% conversion at 170 °C, $V_{reactor}/Q_{feed}$ = 30 min) and the product (**5**) had low solubility in THF leading to fouling at the reactor outlet. Using a 5% MeOH in THF solution resolved the solubility problems, and this small amount of methanol did not lead to measurable amounts of the unidentified impurity previously observed in reactions using 100% MeOH.

The thermal deprotection process was run in a 4.51 mL PFR and then in a 221 mL PFR to produce 1 kg of **5**. Temperature measurements at several points along the length of the 221 mL tube verified that a temperature of >265 °C was reached within <2% of the total reactor length as measured from the oven inlet. The thermal deprotection reaction ran under supercritical fluid conditions at 270 °C at 1000 psig with a measured τ = 9.4 min in the 221 mL PFR.[34] Concentration of the solution to a solid afforded a quantitative yield of **5** of 97% potency. This material was also crystallized from toluene and heptane to afford 79% yield (unoptimized) of **5** with 99.5% potency. In practice, however, the solution of **5** would be used directly in the subsequent step in the chemical process.

Interestingly, the calculated mean residence time for the thermal deprotection was $V_{reactor}/Q_{feed}$ = 15.9 min for this reaction, but the measured τ was just 12.2 min at 210 °C and 9.4 min at 270 °C (40% less than calculated if not correcting for density changes in the reactor). As stated earlier in this paper and remarkably clear in this case, when fluid density and/or physical phase changes occur within the reactor compared to feed solutions, $V_{reactor}/Q_{feed}$ will not equal τ. In this specific case the critical temperature for THF/MeOH was exceeded at 270 °C, resulting in a single-phase fluid with much lower density (0.53 g/mL) vs. that at ambient (0.896 g/mL). At 210 °C which is below the critical temperature, the thermal expansion of the liquid phase results in τ = 12.2 min (Table 5).

Calculating D/uL from the experimental F-curves in both the 4.51 mL (Figure 11) and 221 mL[35] PFRs revealed that elevated temperatures also have a dramatic effect on axial dispersion. The F-curve measurements were made by first flowing solvent only through the tube reactor at the given conditions, then switching from solvent only to a solution of dissolved **5** flowing into the tube, and measuring concentration of **5** vs. time flowing out the end (Figure 11). In the figure, C/C_0 is the ratio of **5** concentration measured in tube effluent, C, divided by concentration of **5** in the solution flowing into the reactor after

Table 5. Impact of temperature on τ, D/uL of substrate 5, *Re*, and density for flow-through 4.51 and 221 mL tube reactors

reactor V (mL)	temp, °C	τ	$D/(uL)$	*Re*	density[a] (g/mL)
4.51	25	13.93	0.0011	24	0.90
4.51	210	10.40	0.0005	121	0.67
4.51	270	8.27	0.0006	ND	0.53
221	25	15.93	0.0026	293	0.90
221	210	12.21	0.0004	1480	0.69
221	270	9.35	0.0004	ND	0.53

[a]Density is the average density for material inside the PFR during steady-state flow conditions, calculated from measured F-curve, numerical solution to calculate τ from F-curve, known V, and measured mass flow rates.

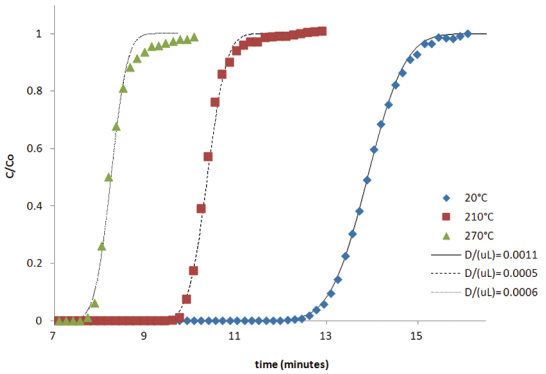

Figure 11. Experimental F-curves and dispersion model fits for transition from solvent-only to dissolved substrate **5** at different temperatures in a 4.51 mL PFR.

the step change, C_o. D/uL decreases from 0.0011 to 0.0005 in the 4.51 mL reactor, and D/uL decreases from 0.0026 to 0.0004 in the 221 mL reactor, when temperature is increased from 20 to 210 °C. D/uL for supercritical conditions at 270 °C was about the same as for 210 °C (Table 5). Definition of D/uL, how it relates to axial dispersion, and calculation of D/uL from experimental F-curves are described in the next section of this paper.

PFR systems are ideally suited to examine the effects of temperature, stoichiometry, concentration, and τ on reaction yield and purity. Combining automated temperature control (GC oven) with the ability to automatically sample and dilute the product stream at the reactor outlet for HPLC assay[36] led to a powerful automated reaction-condition screening setup. In this study we examine the thermal Boc group deprotection of **5** as a 5% solution in *N*-methylpyrrolidinone (NMP) at $V_{reactor}/Q_{feed}$ = 15 min. A GC oven was programmed to heat to a given temperature, hold for a set time (30 min), then heat to a new temperature and hold again. The hold time could be varied to establish a specific duration at each new steady state. The hold time at each temperature was twice the $V_{reactor}/Q_{feed}$ to ensure at least two samples at steady state for every temperature. The automated sampling and diluting system at the outlet provided vials ready for wt % HPLC assay. Once started, the system could run unattended for a specified duration.

dx.doi.org/10.1021/op200351g | *Org. Process Res. Dev.* 2012, 16, 982−1002

A single-feed pump at a single flow rate was used in the first experiment with this system, and therefore one value of $V_{reactor}/Q_{feed}$ could be examined per screen. The GC oven was programmed to ramp from 180 to 260 °C. Aliquots were drawn automatically every 10 min and assayed following the experiment. This sequence ran *completely unattended* overnight, and the data were analyzed the following day.[37] In addition to conversion data (Figure 12) that one might have also used a commercial React-IR

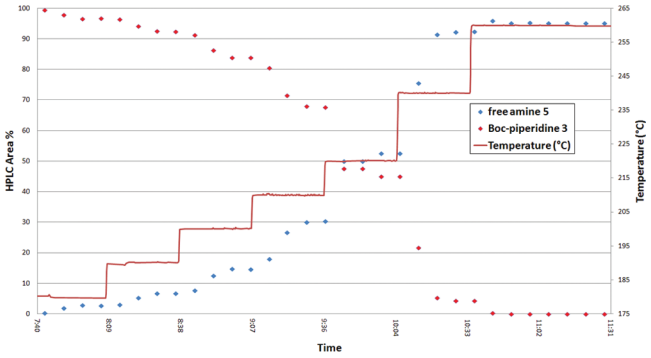

Figure 12. Thermal De-Boc in NMP: automated temperature screening.

system to obtain, the HPLC samples allowed trace impurities to be tracked (Figure 13), something not possible with React-IR. A

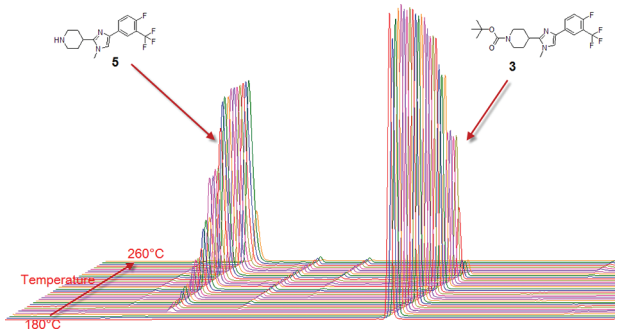

Figure 13. HPLC traces from automated thermal De-Boc temperature screen.

second generation system in which multiple pump flow rates as well as temperatures can be automated has since been developed and increases optimization speed in this reactor setup.

Safety of PFRs. One of the well-established benefits of using a PFR is their inherent safety vs batch reactors. This safety advantage arises from two primary areas, lower reactor volume and superior heat transfer. Reactor volume in a PFR is at least 1 order of magnitude smaller than in a batch reactor for the same throughput, assuming one batch per day vs a continuous reaction running with τ less than 2 h. In addition, heat transfer surface area per unit volume (A/V) is 1−2 orders of magnitude larger. Table 10 shows A/V calculations for each of the PFRs used in this study, which can be compared to A/V for typical batch reactors. The PFR setups used in this paper were all tested at 1.5× the planned operating pressure. The equipment setups were also equipped with pressure reliefs for all positive displacement pumps and for the reactors. For highly exothermic reactions, heat transfer fluid with turbulent mixing or flow was used on the outside of the tube reactor, rather than forced convection for PFR temperature control.

Continuous Reactor Selection and Characterization. In a PFR, residence time distribution can be described by axial dispersion which is well characterized in laminar flow tubes.[38] The extent of dispersion affects the residence time that some molecules are subjected to reaction conditions which can influence impurity profile. Axial dispersion must also be understood as the process is scaled to larger reactors that may have different geometries or operate in different flow regimes. Levenspiel showed that the vessel dispersion number (D/uL) can be used to quantify the extent of dispersion in a given vessel under a set of operating conditions, where D is the Taylor longitudinal dispersion coefficient that incorporates the effects of both diffusion and convection, u is average flow velocity, and L is vessel length. A perfect plug flow reactor would have a $D/uL = 0$, while a perfect continuous stirred tank reactor would have $D/uL = \infty$. Using the guidance of Levenspiel, $D/uL = 0.025$ represents an intermediate amount of dispersion, while 0.002 represents a low amount of dispersion.[39]

As axial dispersion increases, so does the reaction time required for a given fractional conversion. Fractional conversion of reactant A, as it passes through a tubular reactor, is governed by axial dispersion, advection, reaction rate, and reaction order, as shown in the following dimensionless form of the material balance equation for component A (eq 1) where X_A = fractional conversion of reagent A, C_{A0}= initial concentration, z = fraction of total reactor length (l/L), k = reaction rate constant, and n = reaction order.

$$\frac{D}{uL}\frac{d^2X_A}{dz^2} - \frac{dX_A}{dz} + k\tau C_{A_0}^{n-1}(1 - X_A)^n = 0 \quad (1)$$

The impact of dispersion can be clearly seen in Table 6 where τ to reach 99.9% conversion for an isothermal elementary

Table 6. Impact of axial dispersion on reaction time for an elementary first-order reaction that requires 90 min in an ideal PFR

axial dispersion number (D/uL)	τ to reach 99.9% conversion (min)	change vs ideal (%)
0 (ideal)	90	0
0.002 (low dispersion)	91.2	+1.3
0.025 (intermediate dispersion)	105	+17
0.2 (higher dispersion)	196	+117

first order reaction has been calculated at multiple dispersion numbers for a 90 min reaction. If axial dispersion is low ($D/uL = 0.002$), then τ required for 99.9% conversion is about 1.3% longer than ideal PFR, assuming the same reaction conditions. Time to reach 99.9% conversion would be 17% longer with intermediate dispersion ($D/uL = 0.025$) and 117% longer with higher dispersion ($D/uL = 0.2$). Low vessel dispersion numbers ensure that the kinetic results obtained would be well modeled by assuming plug flow reactor models (PFR) and thus neglecting the first term in eq 1. Many reactions that chemists may chose to run in flow are fast (seconds), such as metalation, while others may be accelerated to achieve complete conversion in seconds or minutes by extreme conditions. However, many reactions require longer reaction times (hours) due to slower kinetics or impurity formation under more extreme reaction conditions. In the case of slower reactions, maintaining low axial dispersion is particularly important to minimize the transition time to steady state and minimize τ required for full conversion at temperature that results in highest purity. The extent of axial dispersion also influences impurity profile since some material

dx.doi.org/10.1021/op200351g | Org. Process Res. Dev. 2012, 16, 982−1002

resides in the reactor a longer time and some a shorter amount of time. Maintaining negligible axial dispersion (plug flow) minimizes this effect and can improve impurity profile in certain cases.

Plotting C/C_0 vs t/τ after a step change in nonreactive tracer flowing into a tube produces an S-shaped curve (for example, see Figure 11), where C is nonreactive tracer concentration at exit and C_0 is tracer concentration at the inlet. Dankwerts defined this as the F-curve.[40] It is mathematically equal to the integral of the Dankwerts "C-curve", which is the C/C_0 response curve to a pulse injection of nonreactive tracer. The C-curve and the F-curve are functions of D/uL mathematically; therefore, both may be used to calculate D/uL. The spread of the C-curve as measured by its variance (σ_θ^2) is related to D/uL by the relationship shown in eq 2:[41]

$$\frac{D}{uL} = \frac{1}{8}\left(\sqrt{8\sigma_\theta^2 + 1}\right) - 1 \tag{2}$$

The relationship shown in eq 2 gives a convenient method for quantifying D/uL from experimental F-curve data. In the case of low dispersion the observed concentration change will be normally distributed about a mean. Alternatively, D/uL can be calculated by fitting experimental F-curve data to the basic differential equation representing dispersion by numerically solving for D/uL as shown in eq 3 where θ = dimensionless time (t/τ).

$$\frac{\partial C}{\partial \theta} = \left(\frac{\mathbf{D}}{uL}\right)\frac{\partial^2 C}{\partial z^2} - \frac{\partial C}{\partial z} \tag{3}$$

D/uL was quantified by both methods described above for all coiled tube reactors in this study. The two methods of calculating D/uL from experimental F-curve data agreed within 5% where $D/uL < 0.01$. Where $D/uL > 0.01$, the reported value was calculated by the variance method. All reactors were tested using a 90 min τ as well as 5 min τ to span a typical range of residence times for reactions reported in this paper. For each solvent-only axial dispersion experiment, the F-curve was obtained by making a step change from 100% THF to a 60%/40% (v/v) THF/toluene mixture flowing into the tube, or vice versa, and monitoring the concentration of toluene in the reactor effluent, either by online Raman probe or manual sampling and off-line HPLC analysis. Axial dispersion was measured at both τ = 5 and 90 min for 20 coiled tube reactors, 9 of which were used in this paper (Table 10). The average axial dispersion number for the reactors used in this study was 0.0008, as characterized by the testing with solvents only. Using the mathematical relationships introduced above, the difference between real reactors with D/uL = 0.0008 vs ideal PFRs is about 0.5% longer τ to reach the same fractional conversion. On the basis of this data we refer to the tube reactors in this study as PFRs for practical purposes, rather than PFDRs (plug flow with dispersion reactors).

The data in Table 10 supports that higher L/d leads to lower axial dispersion over the wide range of reactor volumes and residence times shown in the table. Correlations for vessel dispersion numbers have been developed of the general form shown in eq 4.[42]

$$\frac{D}{uL} = (\text{intensity of dispersion})(\text{geometric factor}) \tag{4}$$

The intensity of dispersion is defined as D/ud which has been correlated to the Reynolds number (Re) and Schmidt number (Sc), and for straight tubing the geometric factor is defined as d/L. We more commonly refer to the inverse, L/d. The reactors in this paper were coiled in various geometries, and the geometric factor is certainly more complex than simply d/L. For example, Table 7

Table 7. Impact of coil diameter on axial dispersion

entry	total tube length (m)	d (mm)	coil diameter (m)	D/uL (at τ = 90 min)
1	122	4.57	0.22	0.0010
2	122	4.57	0.43	0.0016

shows that axial dispersion number is slightly lower if the tubing has a smaller coil diameter. Regardless, the trend remains valid that coiled tubes with higher L/d have lower axial dispersion, for about the same reactor V and τ (Table 8). For

Table 8. Impact of L/d on axial dispersion

average V (mL)	V (mL)	L/d	D/uL (at τ = 90 min)	D/uL (at τ = 5 min)
1.8	1.75[a]	12,773	0.0003	0.0017
	1.84	435	0.0065	0.0088
25	20.5[a]	149,587	0.0005	0.0004
	28.8	9,822	0.0010	0.0023
	25.5	1,714	0.0013	0.0098
700	682	105,813	0.0003	0.0005
	776	10,336	0.0013	0.0039
	632	3,106	0.0047	0.0049
1900	1462[a]	226,990	0.0002	0.0001
	2003	26,684	0.0016	0.0025
	2185	3,194	0.0091	0.0031
8000	7140[a]	19,553	0.0008	0.0002
	8726	2,845	0.0385	0.0019

[a]Coiled tube reactor used for running chemistries reported in this paper.

more details on these coiled tube reactors, see Table 10 for complete characterization.

The impact of L/d is more dramatic for larger PFRs at longer τ. These results can be explained with existing textbook correlations,[42] because D/uL is the product of d/L and D/ud, and D/ud is a function of Re and Sc numbers with existing correlations. For a given D/ud, Re and Sc, one way to decrease D/uL is to decrease d/L. We opted for a conservative approach, designing the reactors with high L/d in research and development experiments when τ required to maximize conversion and minimize impurities is initially unknown.[43]

Interestingly, there was less axial dispersion at slower flow rates for the smaller tubes in the laminar flow regime, but there was more axial dispersion at slower flow rates for the larger tubes. F-curves for the smallest and largest reactor used for chemistries reported in this paper are respectively shown in Figures 14 and 15. The figures show that the impact of τ on D/uL reverses when we go from a 1.75 to a 7140 mL coiled tube.

Higher L/d also leads to faster characteristic mixing time by diffusion, which is more important for the small-diameter laminar flow tubes used in this study. For streamline laminar flow in tubes, radial mixing is adequate compared to longitudinal mixing to ensure a sufficiently uniform cross-sectional concentration of material if the following relationship holds (eq 5, Taylor criterion for sufficient radial mixing by diffusion alone) is attained where D_v is the molecular diffusion coefficient.

$$\frac{L}{u} \gg \frac{d^2}{28.8D_v} \tag{5}$$

dx.doi.org/10.1021/op200351g | Org. Process Res. Dev. 2012, 16, 982−1002

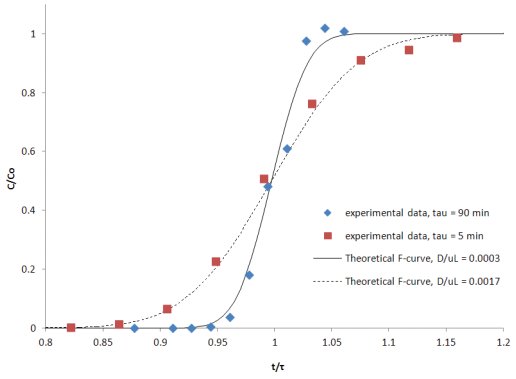

Figure 14. Experimental F-curves and dispersion model fits for 1.75 mL tube reactor for τ = 5 and 90 min.

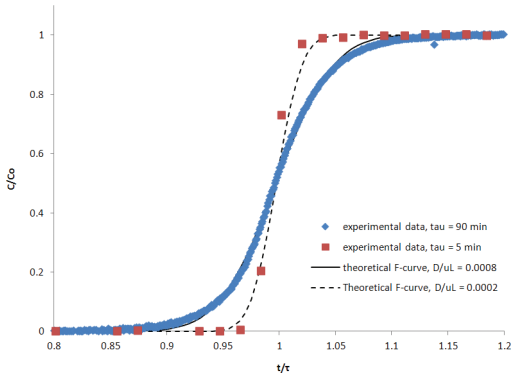

Figure 15. Experimental F-curves and dispersion model fits for 7140 mL tube reactor for τ = 5 and 90 min.

Ideal plug flow behavior is defined by complete mixing in the radial direction but no mixing in the axial direction. Therefore, velocity profiles in the axial direction must be overcome by radial mixing to approach plug flow behavior. Mixing in the radial direction at large scale is dominated by turbulence as represented by *Re*, but mixing in the radial direction at smallest scale in laminar flow tube reactors is dominated by diffusion. In the smaller-diameter tubes in the laminar flow regime, axial dispersion is lower at longer τ, despite the fact that *Re* is lower (Table 9). This is observed since longer τ gives more time for radial diffusion and compensates for parabolic velocity profiles in the longitudinal direction.[42] In contrast, in the larger-diameter tube reactors, where diffusion path in the radial direction is much longer and thus diffusion has less impact on radial mixing, axial dispersion is lower at higher *Re* (Table 9).

Table 9. Impact of Reynolds number on axial dispersion

V (mL)	*d* (mm)	*Re* (at τ = 90 min)	*Re* (at τ = 5 min)	*D*/*uL* (at τ = 90 min)	*D*/*uL* (at τ = 5 min)
1.75	0.56	1.2	22	0.0003	0.0017
221	1.96	45	809	0.0005	0.0024
776	4.57	67	1215	0.0013	0.0039
2185	9.55	91	1637	0.0091	0.0031
7140	7.75	367	6598	0.0008	0.0002
8726	15.7	220	3967	0.0385	0.0019

Higher *L*/*d* also leads to more isothermal reaction conditions. The criterion for isothermal performance of a tubular reactor in the laminar flow regime is given by the following constraint on tube diameter (eq 6, Hickman criterion for isothermal performance of tubular reactor).[44] Thus, smaller inner diameter leads to more isothermal characteristics for laminar flow tubular reactors, as one would expect intuitively.

$$d^2 \leq \frac{14kR_gT_w^2}{R_{max}(-\Delta H)(20E_a - R_gT_w)} \quad (6)$$

where:
k=thermal conductivity of the reaction fluid (W m^{-1} K^{-1})
R_g=universal gas constant (8.314 J mol^{-1} K^{-1})
T_w=wall temperature (K)
R_{max}=reaction rate maximum (mol m^{-3} s^{-1})
ΔH=heat of reaction (J mol^{-1})
E_a=activation energy (J mol^{-1})

One practical limit to higher *L*/*d* is pressure drop. Hagen–Poiseuille calculations for laminar flow in tube reactors,[45] as well as measured pressure drop from the axial dispersion tests at two flow rates are shown in Table 10. Average pressure drop for solvents flowing in the tube reactors used in this study was 5 psi for τ = 90 min, and 100 psi for τ = 5 min. Most reactions used by the pharmaceutical industry have longer reaction times, which allow for high *L*/*d* PFRs with manageable pressure drop.

CONCLUSIONS

In conclusion we have demonstrated two different synthetic approaches to 1*H*-4-substituted imidazole **5**. Both approaches utilized PFRs for reaction optimization and scale up. The first generation approach highlighted how continuous technologies can be used to rapidly screen conditions and accelerate early phase material delivery. Rapid heat up with PFR technology allowed for the preparation of large-scale quantities of **2** in spite of challenging starting material degradation kinetics. A pilot plant-scale process in a 7.1 L PFR was described where 58 kg of ketoamide **1** was processed through the key cyclization reaction under cGMP conditions in a lab hood infrastructure. The results in the PFR were superior to what could have been obtained in batch equipment at this scale. The second generation effort highlighted an improved route to imidazole **5** via *N*-methylketoamide **6**. This approach highlighted a superior thermal cyclization reaction and efficient and environmentally friendly thermal Boc group deprotection reactions in PFRs. Automated sampling and dilution for HPLC analysis allowed for data-rich experimentation which led to faster development and scale up. The cyclization of *N*-methylketoamide **6** and thermal deprotection reaction were both demonstrated in PFRs at 1 kg scale. The deprotection was accomplished under supercritical fluid conditions in the flow reactor, which allowed for a single homogeneous phase even though CO_2 and isobutylene were evolved. The throughput advantages in this chemistry also point to the possibility of achieving low volume (1–2 MT) commercial scale throughput safely in a laboratory hood infrastructure. PFRs represent excellent cost-effective research tools for screening temperature, extreme conditions, time, stoichiometry, but not necessarily reagents or solvents. Overall, nine different PFR reactor sizes were used in the course of this work. The high surface area per unit volume, high pressure rating of tubes (vs tanks), and the smaller size required for a given kg/day throughput make the

dx.doi.org/10.1021/op200351g | Org. Process Res. Dev. 2012, 16, 982–1002

Table 10. Dimensions and characterization of coiled tubular PFRs

Dimensions and Dispersion[a]							
entry	V (mL)	o.d. (mm)	d (mm)	L (m)	L/d	D/uL (at τ = 90 min)	D/uL (at τ = 5 min)
1[b]	1.75	1.59	0.56	7.14	12,773	0.0003	0.0017
2	1.84	3.18	1.75	0.76	435	0.0065	0.0088
3[b]	2.40	1.59	0.56	9.79	17,517	0.0002	0.0015
4	3.68	3.18	1.75	1.52	870	0.0035	0.0063
5[b]	4.51	1.59	0.56	18.4	32,918	0.0004	0.0010
6	17.0	3.18	2.67	3.05	1,143	0.0020	0.0081
7[b]	20.5	1.59	0.56	83.6	149,587	0.0002	0.0004
8	25.5	3.18	2.67	4.57	1,714	0.0013	0.0098
9	28.8	3.18	1.55	15.2	9,822	0.0010	0.0023
10[b]	143	3.18	1.96	47.6	24,344	0.0010	0.0024
11[b]	221	3.18	1.96	73.6	37,622	0.0005	0.0024
12[b]	541	3.18	2.02	169	83,974	ND	ND
13	682	3.18	2.02	213	105,813	0.0003	0.0005
14	776	6.35	4.57	47.3	10,336	0.0013	0.0039
15	632	9.53	6.38	19.8	3,106	0.0047	0.0049
16[b]	1462	3.18	2.02	458	226,990	0.0002	0.0001[d]
17	2003	6.35	4.57	122	26,684	0.0010	ND
18	2003	6.35	4.57	122	26,684	0.0016	0.0025
19	2185	12.70	9.55	30.5	3,194	0.0091	0.0031
20[b]	7140	9.53	7.75	151	19,553	0.0008	0.0002
21	8726	19.05	15.7	44.8	2,845	0.0385	0.0019

Characterization[c]								
entry	Re (at τ = 90 min)	Re (at τ = 5 min)	measured pressure drop (psi, at τ = 5 min)	calculated pressure drop (psi, at τ = 5 min)	measured pressure drop (psi, at τ = 90 min)	calculated pressure drop (psi, at τ = 90 min)	A/V (m^2/m^3)	number of coils
1[b]	1.2	22	0	1	0	0.07	7158	20
2	0.4	7.5	0	0.002	0	0	2282	2.0
3[b]	1.7	31	0	2	0	0.1	7158	27
4	0.8	15	0	0.006	0	0	2282	1.6
5[b]	3.2	58	6	9	2	0.5	7158	65
6	2.5	46	0	0.01	0	0	1500	2.9
7[b]	15	263	160	180	9	10	7158	131
8	3.8	69	0	0.02	0	0.001	1500	4
9	7.4	133	0	0.8	0	0.04	2577	55
10[b]	29	524	4	5	1	0.3	2045	43
11[b]	45	809	10	11	1	0.6	2045	88
12[b]	ND	ND	ND	ND	ND	ND	1983	ND
13	134	2420	226	90	4	5	1983	396
14	67	1215	0	0.9	0	0.05	875	67
15	40	710	0	0.08	0	0.004	627	12
16[b]	288	5191	497[d]	415	25	23	1983	675
17	174	3136	13	6	0	0.3	875	180
18	174	3136	14	6	0	0.3	875	90
19	91	1637	0	0.08	0	0.005	419	18
20[b]	367	6598	28	3	1	0.2	516	119
21	220	3967	0	0.07	0	0.004	254	17

[a] V is tube volume, o.d. is tube outer diameter, d is tube inner diameter, L is tube length, D/uL is vessel dispersion number. [b] Coiled tube reactor used for running chemistries reported in this paper. [c] Re is Reynolds number for solvent tests at room temperature; A/V is heat transfer surface area per unit volume. [d] Planned τ was 5 min, but actual τ was 9.45 min.

PFRs intrinsically safer than batch processing for the thermal reactions described herein. The ability to access extreme conditions in these reactors expanded the design space compared to conventional laboratory and scale-up equipment. D/uL for the nine coiled tube reactors used in this study averaged 0.0008 and ranged from 0.0001 to 0.0024, as characterized by testing with solvents only at τ = 5 and 90 min. Therefore axial dispersion is negligible and the tubes can be modeled as PFRs with errors less than 2% between the actual and the theoretically ideal.

EXPERIMENTAL SECTION

Materials. Starting materials, solvents, and reagents were purchased commercially and used without further purification unless otherwise indicated. HPLC analysis performed using Agilent 1100 HPLC system unless otherwise indicated. ^{1}H NMR, ^{19}F, and ^{13}C NMR spectra were obtained on a Varian spectrometer at 400 and 100 MHz and calibrated using residual undeuterated solvent as an internal reference. The following abbreviations were used to explain the multiplicities: s = singlet,

dx.doi.org/10.1021/op200351g | Org. Process Res. Dev. 2012, 16, 982−1002

d = doublet, t = triplet, q = quartet, quin = quintuplet, m = multiplet, br = broad. IR spectra were obtained on a Smiths ChemID FTIR and high-resolution MS data was acquired on an Agilent G1969A MS-TOF. Melting points were taken on a DSC Q1000 machine or obtained via DSC analysis. The dimensions of the PFR reactors used in this paper are as follows in Table 10. All reactors were constructed with 316 L SS.

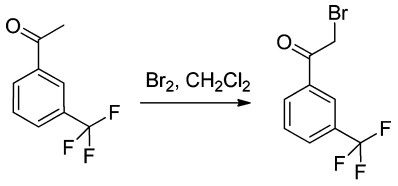

7a

2-Bromo-1-(3-trifluoromethyl-phenyl)ethanone[46] (7a). To a 22 L four-necked round-bottom flask (fitted with addition funnel, nitrogen blanket, condenser, scrubber, and mechanical stirrer) was added 3-trifluoromethylacetophenone (1500 g, 1.00 equiv, 7.97 mol) and dichloromethane (7.5 L). The resulting clear, colorless solution was stirred at room temperature while adding a solution of bromine (1274 g, 1.00 equiv, 7.97 mol) in dichloromethane at room temperature via addition funnel over 4 h. After sampling to determine reaction completion by GC[47] the reaction was quenched by slow addition of saturated aqueous $NaHCO_3$ (2000 mL), controlling the temperature by ice bath to less than 25 °C. The phases were separated, and the organic layer washed with brine (2000 mL); the solution was then dried over sodium sulfate, filtered, and concentrated on a rotovapor to a clear colorless oil. This crude oil, containing the product plus 7−8% each of the starting acetophenone and dibrominated byproduct, was purified by silica gel chromatography (silica gel; step gradient, 20% to 50% CH_2Cl_2 in heptane) to afford bromide **7a** (1667 g, 6.24 mol, 78%) as a clear, colorless oil (100% purity by GC). ^{1}H NMR (400 MHz, $CDCl_3$) δ 8.24 (s, 1H), 8.17 (d, 1H, J = 8.4 Hz), 7.87 (d, 1H, J = 8 Hz), 7.66 (t, 1H, J = 8 Hz), 4.46 (s, 2H)

(2-Amino-1-(3-trifluoromethyl-phenyl)-ethanone)-, *p*-Toluene Sulfonate (15a). Bromide **7a** (1664.7 g, 1.00 equiv, 6.23 mol) and tetrahydrofuran (7500 mL) were charged to a 12 L three-necked RBF fitted with water-cooled condenser, nitrogen blanket, mechanical stirrer, and cooling bath. Sodium azide (425.6 g, 1.05 equiv, 6.55 mol) was charged in one portion as a solid along with water (135 mL). The pale-yellow slurry was stirred at room temperature under nitrogen. After 6 h, water (260 mL) was added, and the mixture was stirred overnight. The resulting orange slurry was then filtered over a thin pad of Celite and rinsed with THF (1 L). The resulting solution of intermediate azide was divided into two equal portions (5146.5 g each) for side-by-side reductions. Two identical 22 L three-necked RBFs (fitted with addition funnel, water-cooled condenser, nitrogen blanket, mechanical stirrer, and cooling bath) were charged with triphenylphosphine (889 g, 3.43 mol, 1.1 equiv), *p*-toluene sulfonic acid monohydrate (1304 g, 6.86 mol, 2.2 equiv), and THF (5.6 L). The two portions of intermediate azide mixture were added via addition funnels to the individual flasks over 4 h, controlling the foaming from nitrogen evolution by addition rate and the temperature to <20 °C by use of an ice bath. *CAUTION: Vigourous gas evolution occurred during this addition.* On completion of addition the slurry was stirred at ambient temperature for 2 h, and then the solids were filtered from both reactors onto the same filter. Both flasks and the combined cake were washed with THF (4 L). The solids were dried in a vacuum oven at 40 °C overnight to afford 2340 g (72%) of (2-amino-1-(3-trifluoromethyl-phenyl)-ethanone)-, *p*-toluene sulfonate (1:1) as a white, crystalline solid (mp 197 °C). ^{1}H NMR (400 MHz, DMSO-d_6) δ 8.24−8.30 (m, 5H), 8.09 (d, 1H, J = 8 Hz), 7.83 (t, 1H, J = 8 Hz), 7.46 (d, 2H, J = 6.4 Hz), 7.08 (d, 2H, 7.6 Hz), 4.69 (brs, 2H), 2.26 (s, 3H); ^{19}F NMR (376.2 MHz, DMSO-d_6) δ −61.273 (s, 3F); IR (KBr, ν/cm^{-1}) 3154, 2998, 2905, 1703, 1495, 1331, 1225, 1172, 1115, 812, 694, 555. Elem. Anal.: Calcd for $C_{16}H_{16}F_3NO_4S$: C, 51.20%; H, 4.30%, N, 3.73%. Found: C, 51.24%; H, 4.39%, N, 4.00%.

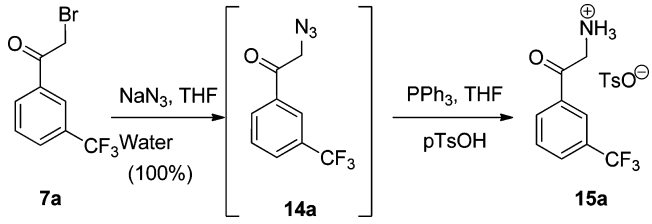

7a 14a 15a

4-[2-Oxo-2-(3-trifluoromethyl-phenyl)-ethylcarbamoyl]-piperidine-1-carboxylic Acid *tert*-Butyl Ester (11a). Amine salt **15a** (913 g, 2.43 mol) and **10** (623 g, 2.73 mol, 1.12 equiv) along with THF (2.75 L) and EtOAc (5.5 L) were combined in a 22 L three-necked RBF fitted with water-cooled condenser, nitrogen blanket, mechanical stirrer, and cooling bath flask. The reaction was cooled to 0−5 °C with an ice bath. T3P (1.2 equiv, 2.91 mol, 1.512 L of a 50% solution in EtOAc) was added over 15 min and the reaction temperature maintained at 0−5 °C during addition. After stirring for 10 min *N*-methylmorpholine (566 g, 5.6 mol, 2.3 equiv) was added over 30 min, holding the temperature below 5 °C during addition. The reaction was warmed to room temperature, and once deemed complete (<5% **15a** by HPLC, usually after 10 h), the mixture was cooled in an ice bath, and water (7.3 L) was added rapidly. The layers were separated, and the aqueous layer was washed with EtOAc (2.75 L). The organic layers were combined and washed with 0.5 M aqueous sodium bicarbonate solution (2.75 L). The organic layer was washed with brine solution (2.75 L), and the resulting organic layer was then treated with sodium sulfate and filtered. The solvent was removed via atmospheric distillation down to ∼4.6 L. Heptane (11 L) was added while removing solvent via distillation until the final volume reached ∼11 L. The mixture was cooled to 50 °C and seeded. The resulting slurry was held at 50 °C for 3 h and then cooled to room temperature and stirred for 2 h. The solids were filtered, and the cake was washed, first with 10% EtOAc in heptane (2 L) and then with heptane (2 L). After drying in a vacuum oven at 60 °C for 3 h, 800 g (79%) of

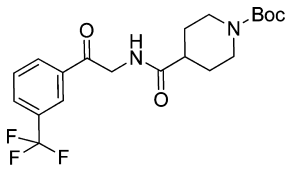

11a

ketoamide **11a** was obtained as a white solid (mp 116 °C). ^{1}H NMR (500 MHz, DMSO-d_6) δ 8.30 (t, 1H, J = 5.5 Hz), 8.25 (d, 1H, J = 7.5 Hz), 8.21 (s, 1H), 8.03 (d, 1H, J = 7.5 Hz), 7.79 (t, 1H, J = 7.5 Hz), 4.61 (d, 2H, J = 5.5 Hz), 3.91 (d, 2H, J = 12.5 Hz),2.75 (brs, 2H), 2.40−2.51 (m, 1H), 1.66 (dd, 2H,

dx.doi.org/10.1021/op200351g | Org. Process Res. Dev. 2012, 16, 982−1002

J = 13.5, 3 Hz), 1.30−1.44 (m, 9H); ^{19}F NMR (376.2 MHz, DMSO-d_6) δ −61.342 (s, 3F); IR (KBr, ν/cm^{-1}) 3229, 3011, 2942, 2851, 1642, 1544, 1429, 1368, 1160, 1066, 805, 690; HRMS (ESI): calc'd for $C_{20}H_{25}O_4N_2F_3{}^{23}Na_1$ = 437.1659, found 437.1647; See Supporting Information for HPLC chromatogram.

(4-[4-(3-Trifluoromethyl-phenyl)-1*H*-imidazol-2-yl]-piperidine)-, dihydrochloride (13a). A solution of ketoamide **11a** (773.3 g, 1.00 equiv, 1.87 mol) in methanol (2300 mL) was prepared. (Total solution volume = 2900 mL, [s.m.] = 1.87 mol/2.90 L = 0.645 M.) A separate solution of ammonium acetate (755.08 g, 9.80 mol) in methanol (3500 mL) was prepared. (Total solution volume = 4137 mL, {NH_4OAc] = 9.80 mol/4.137 L = 2.367 M.) See Figure 1 for a representation of the reactor setup. Ketoamide **11a** solution was pumped at 5.088 mL/min and the NH_4OAc solution at 6.932 mL/min, resulting in a 5:1 mol ratio of NH_4OAc to **11a**. The two streams were combined in a tee at room temperature and then allowed to flow into the thermal tube reactor described below with the oven temperature at 170 °C. The total time required to process all of the starting material at these flow rates was approximately 5 h.

Desired $V_{reactor}/Q_{feed}$ was 45 min in the 541 mL tube reactor, so total flow rate = 12.02 mL/min was calculated. Reaction profile was periodically monitored by HPLC throughout the 5 h run time. Typical steady-state reaction mixtures contained <1% **11a**, ∼25% **13a freebase** resulting from thermal deprotection and ∼75% **12**.

All of the collected product solution was combined and concentrated on rotovap and solvent exchanged into 3500 mL of *n*-BuOH. This solution was washed with a mixture of 3000 mL of sat'd aqueous $NaHCO_3$ and 1000 mL water. This *n*-BuOH sol'n was then washed with sat'd aqueous NaCl (3000 mL) followed by azeotropic drying by distillation of 1 L of *n*-BuOH on the rotovapor (45 °C bath temp). The solids (NaCl) that precipitated during distillation were filtered, and the filtrate was charged to a 5 L four-neck flask in a cooling bath. Anhydrous HCl (g) was bubbled slowly into the solution, controlling the temperature <55 °C with and ice−water bath. Solids precipitated during the HCl gas addition. Reaction progress was monitored by HPLC until <0.5% of the Boc-protected intermediate remained. On completion of reaction heptane (4000 mL) was added slowly via addition funnel, and the resulting slurry was cooled to <5 °C in an ice bath and held for 15 min. The solids were filtered, and the cake was washed with heptane (2 × 600 mL). Solids were dried in a 40 °C vacuum oven to afford 619.1 g (92%) of imidazole salt **13a** as a white solid; ^{1}H NMR (400 MHz, DMSO-d_6) δ 9.28−9.21 (s, 1H), 9.20−9.12 (s, 1H), 8.34 (s, 1H), 8.26−8.25 (m, 2H), 7.76−7.70 (m, 2H), 3.49−3.43 (m, 1H), 3.37 (q, J = 6.4 Hz, 2H), 3.08−2.99 (m, 2H), 2.30 (d, J = 12.3 Hz, 2H), 2.16−2.05 (m, 2H); IR (KBr, ν/cm^{-1}) 2492, 2132, 1703, 1569, 1454, 1339, 1286, 1168, 1123, 956, 694, 547; HRMS (ESI): calcd for $C_{15}H_{17}N_3F_3$ = 296.1369, found 296.1360; See Supporting Information for HPLC chromatogram.

(2-Amino-1-(4-fluoro, 3-trifluoromethyl-phenyl)-ethanone)-, *p*-Toluene Sulfonate (15b). To a 1000 L glass-lined reactor was added THF (350.0 kg) while maintaining a temperature range of 15−25 °C. Bromide **7b** (78.5 kg) was then added to the reactor. The mixture was cooled to −2 to 2 °C, and an aqueous solution of sodium azide (prepared with sodium azide (19.7 kg) and purified water (62.8 kg)) was added to the mixture at the rate of 15−20 L/h. The reaction was sampled every hour and analyzed by HPLC for completion (<0.5% **7b**). After stirring 10 h at −2−2 °C the reaction was deemed complete by HPLC. The stirring was stopped, and the layers were allowed to settle for 30 min before removing the aqueous phase. The resulting crude solution of azide **14b** was used without isolation in the next unit operation.

In a separate 3000 L reactor were added THF (351 kg), triphenylphosphine (86.7 kg), and *p*-toluene sulfonic acid (104.8 kg) in sequence. The mixture was stirred for 30 min at room temperature. The crude solution of azide **14b** was added to the reactor at a rate (30−40 L/h) to maintain an internal temperature between 20 and 25 °C. *The addition rate also controlled the extent of nitrogen off-gassing.* The product (**15b**) crystallizes from solution during this time to form a slurry. After the mixture was stirred 22.5 h azide intermediate **14b** was still present at >0.2%. Additional triphenylphosphine (3.6 kg in 9.6 kg THF) was added to the mixture; 3 h later, the reaction contained <0.2% of azide **14b**.

Then, maintaining the temperature at 20−25 °C, purified water (7.9 kg) was added to quench the reaction at the rate of 10 kg/h. The slurry was stirred for 1 h and then was cooled to 0−5 °C and stirred for 3 h. The mixture was filtered by centrifuge, and the cake was washed twice with THF (209.6 kg × 2) which was cooled to 0−5 °C in advance. The filter cake was dried at 50−55 °C until the water content was <0.5% and LOD <0.5%. **15b** (97 kg, 89.6%, 99.7% purity) was obtained as an off-white solid. Amine salt **15b**: White crystalline solid, mp 212−219 °C. ^{1}H NMR (399.84 MHz, DMSO-d_6) δ 8.40−8.36 (m, 1H), 8.32−8.27 singlet-broad, 3H), 7.78−7.73 (m, 1H), 7.45 (d, J = 8.3 Hz, 2H), 7.08 (d, J = 7.5 Hz, 2H), 4.68 (s, 2H), 2.26 (s, 3H).

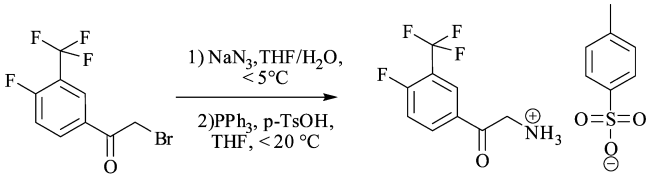

^{19}F NMR (376.2 MHz, DMSO-d_6) δ −60.324 (d, J = 11.99 Hz, 3F), −107.17 (m, 1F); HRMS (ESI): calcd for $C_9H_8F_4NO$ = 222.0537, found: 222.0531; IR (KBr, ν/cm^{-1}) 3436, 2913, 1669, 1621, 1503, 1327, 1254, 1172, 1037, 1008, 816, 666; Elem. Anal.: calcd for $C_{16}H_{15}F_4NO_4S$: C, 48.86%; H, 3.84%, N, 3.56%. Found: C, 48.89%; H, 3.88%, N, 3.63%

4-[2-Oxo-2-(4-fluoro, 3-trifluoromethyl-phenyl)-ethyl-carbamoyl]-piperidine-1-carboxylic Acid *tert*-Butyl Ester (11b). To a 1000 L glass-lined reactor was added ethyl acetate (416.9 kg) while maintaining an internal temperature of 20−25 °C. The mixture was then sampled to measure the water content. An additional portion of THF (104.7 kg) was then

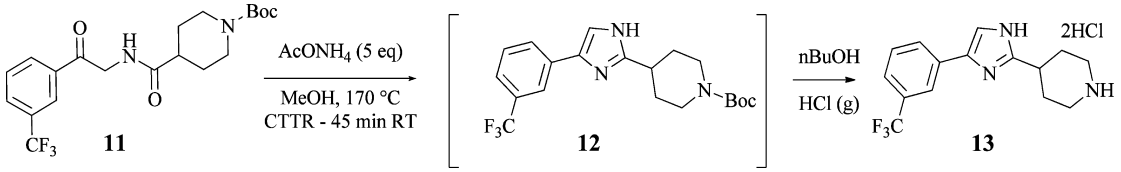

dx.doi.org/10.1021/op200351g | Org. Process Res. Dev. 2012, 16, 982−1002

added. Carboxylic acid **10** (40.6 kg) was added to the mixture under nitrogen gas, and the contents were stirred for 0.5−1 h until all the solids dissolved. Stirring was stopped, and the reactor was evacuated to <0.06 MPa and refilled with nitrogen gas to reach ambient pressure (repeated three times). Stirring was restarted, and 1,1′-carbonyldiimidazole (31.1 kg) was added to the mixture under the protection of nitrogen gas at 20−25 °C. The reaction was stirred for 30 min before 2627394 (58.0 kg) was added to the mixture followed by *N*-methylmorpholine (37.4 kg) at a rate of 6−8 kg/h. The reaction was stirred 16.5 h at 20−25 °C. The reaction was considered complete when the assay yield was >78% and the purity of **11b** was >85%.

Maintaining the temperature at 20−30 °C, water (290.0 kg) was charged to a clean glass-lined reactor. Then the reaction mixture was added to the water and stirred for 10 min. Stirring was stopped, and the mixture was allowed to settle for 30 min before the aqueous phase was removed. Ethyl acetate (52.2 kg) was added to the aqueous phase and was stirred for 30 min. The phases were allowed to separate over 30 min, and the aqueous phase was removed. The combined organic phases were washed with aqueous citric acid (23.3 kg of citric acid and 208.8 kg of water) for 30 min before allowing the phases to separate (30 min). The organic phase was then washed with brine solution (145.1 kg) for 30 min before allowing the layers to separate (30 min). The organic layer was then concentrated to 140−150 L under reduced pressure (0.085 MPa) while maintaining the temperature below 35 °C. The mixture was cooled to 30 °C over 2−3 h, then cooled to −3 to 3 °C for 7 h for crystallization. The mixture was filtered by centrifuge. While the temperature was maintained at 20−30 °C, the filter cake was washed with *n*-heptane (78.9 kg) and dried at 40−45 °C for 23 h. This afforded ketoamide **1** (46.7 kg; 73.2% yield) as an off-white solid in 99.5% purity by HPLC. **11b:** white solid, mp 141−144 °C; ^{1}H NMR (399.84 MHz, DMSO-d_6) δ 8.35−8.31 (m, 1H), 8.29−8.24 (m, 2H), 7.71−7.66 (t, 1H), 4.59 (d, J = 5.7 Hz, 2H), 3.89 (d, J = 12.7 Hz, 2H), 2.74−2.63 (m, 2H), 2.44−2.37 (m, 1H), 1.65 (dd, J = 2.6, 13.2 Hz, 2H), 1.37 (s, 9H); ^{19}F NMR (376.2 MHz, DMSO-d_6) δ −60.324 (d, J = 12.18 Hz, 3F), −108.936 (m, 1F); IR (KBr, ν/cm^{-1}) 3146, 2946, 1675, 1618, 1503, 1417, 1368, 1323, 1279, 1242, 1050, 841, 666; Elem. Anal.: calcd for $C_{20}H_{24}F_4N_2O_4$: C, 55.55%; H, 5.59%, N, 6.48%. Found: C, 55.50%; H, 5.46%, N, 6.50%;

***tert*-Butyl 4-(4-(4-fluoro-3-(trifluoromethyl)phenyl)-1*H*-imidazol-2-yl)piperidine-1-carboxylate (2).** A solution was prepared by combining ketoamide **11b** (55.175 kg, 127.7 mol), ammonium acetate (110.25 kg, 1430.33 mol, 11 equiv), and methanol 580 L). The reactor used for this transformation was a coiled stainless steel tube with 7.75 mm i.d. and 7.14 L volume (Table 10) that was heated in an oven[48] to 140 °C. The back pressure in this tube was controlled at 640 psig by a regulator to allow superheating of the solution above its normal boiling point. The solution prepared above was pumped continuously (using high pressure syringe pumps equipped with automated valve switching packages to allow continuous pumping and refill) through the heated tube under pressure at 79.6 mL/min ($V_{reactor}/Q_{feed}$ = 90 min). As the solution exited the oven, it was cooled back to 20 °C in a tube-in-tube heat exchanger.

Once the entire solution had been processed through the reactor (72 h total processing time), the resulting orange solution was split into two equal sections for workup as follows:

The solution was concentrated under vacuum (50−75 mmHg at 15−30 °C) to a total volume of 165 L. Acetonitrile (60 L) was then added and the solution heated to 50 °C. Water (185 L) was added slowly with seeding over 1 h to crystallize the product. The resulting slurry was stirred at 50 °C for 1 h and then cooled to 20 °C and stirred for 2 h. The solids were filtered and washed with 20% MeOH in water (2 × 65 L). The resulting solids were dried under vacuum at 50 °C.

The dried, crude solids from both sections above were then combined and reslurried in acetonitrile (155 L) at 50 °C. The slurry was cooled to ambient temperature, and the solids were filtered and washed with acetonitrile (120 L) to afford imidazole **2** (29.20 kg, 70.6 mol, 52.5% yield- potency corrected) as an off-white solid (mp 199−202 °C). ^{1}H NMR (399.84 MHz, DMSO-d_6) δ 11.96 (s, 1H), 8.03 (d, J = 6.6 Hz, 2H), 7.67 (s, 1H), 7.44 (t, J = 9.9 Hz, 1H), 3.97 (d, J = 13.2 Hz, 2H), 2.91−2.83 (m, 3H), 1.88 (dd, J = 2.4, 13.0 Hz, 2H), 1.62−1.51 (m, 2H), 1.39 (s, 9H); ^{19}F NMR (376.2 MHz, DMSO-d_6) δ −61.186 ppm: two imidazole tautomers observed in a 12:1 ratio: major tautomer δ −60.01 (d, J = 11.99 Hz, 3F), −120.642 (m, 1F); minor tautomer δ −59.96 (d, J = 12.00 Hz, 3F), −119.575 (m, 1F); IR (KBr, ν/cm^{-1}) 3199, 3109, 2953, 2917, 2856, 1654, 1540, 1442, 1344, 1131, 833, 763, 677; Elem. Anal.: calcd for $C_{20}H_{23}F_4N_3O_2$: C, 58.11%; H, 5.61%, N, 10.16%. Found: C, 58.14%; H, 5.64%, N, 10.20%; HRMS (ESI): calcd for $C_{20}H_{23}F_4N_3O_2$ 414.1799, found 414.1792.

***tert*-Butyl 4-(4-(4-fluoro-3-(trifluoromethyl)phenyl)-1-methyl-1*H*-imidazol-2-yl)piperidine-1-carboxylate (3).** Compound **2** (35 kg, 84.66 mol) was dissolved in dimethyl sulfoxide (455 L). KOH (85%, powdered) (7.99 kg, 121.0 mol, 1.42 equiv) was added in one portion. The result was a thin slurry. Methyl iodide (12.6 kg, 88.77 mol, 1.05 equiv) was charged over 30−60 min pump, maintaining temperature <30 °C. The resulting solution was stirred at 25−30 °C for 1 h or until **2** was consumed to <3% area by HPLC.

A mixture of **3** seed crystals (0.07 kg) and water (105 L) was added over 10−20 min to saturate the solution. The resulting thin slurry was allowed to stir at 25 °C for 20−40 min, at which time the slurry thickened. Additional water (315 L) was then added over 60 min at 23−27 °C to complete the crystallization. The solids were filtered and washed with 20% DMSO in water (2 × 52.5 L and 1 × 105 L) and then dried under vacuum at 60 °C. The resulting dried solids were dissolved in ethanol (245 L) at 50 °C. Water (97.7 L) was then added over 5 min. Seed crystals of **3** (0.065 kg) were then added, and more water (97.7 L) was added over 30−45 min to complete the crystallization. The resulting slurry was cooled to 25 °C over 2 h. The solids were filtered, and the cake was washed with 20% EtOH in water (2 × 83 L). The solids were dried under

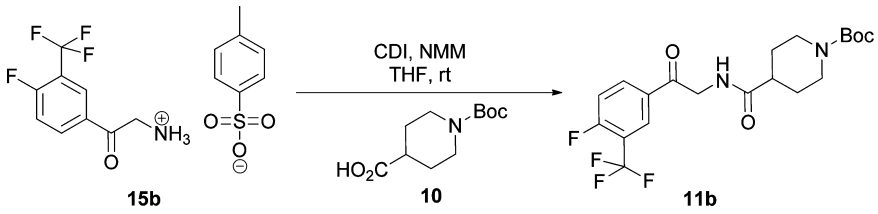

dx.doi.org/10.1021/op200351g | Org. Process Res. Dev. 2012, 16, 982−1002

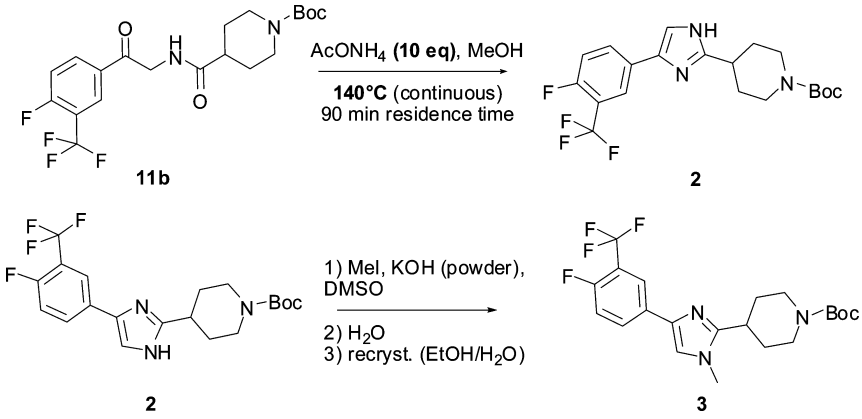

vacuum at 60 °C, affording 31.10 kg (72.76 mol, 86%) of methyl imidazole **3** as a white solid (mp = 199−202 °C). ^{1}H NMR (399.84 MHz, $CDCl_3$) δ 7.93−7.87 (m, 2H), 7.15 (d-d, 1H), 7.06 (s, 1H), 4.24−4.22 (m, 2H), 3.65 (s, 3H), 2.88−2.80 (m, 3H), 2.00−1.84 (m, 4H), 1.71−1.61 (m, 3H), 1.47 (s, 9H); ^{19}F NMR (376.2 MHz, DMSO-d_6) δ −61.37 (d, J = 12.57 Hz, 3F), −118.38 (m, 1F); IR (KBr, ν/cm^{-1}) 3436, 2938, 1679, 1425, 1364, 1336, 1262, 1237, 1160, 1123, 914, 829, 690; Elem. Anal.: calcd for $C_{21}H_{25}F_4N_3O_2$: C, 59.01%; H, 5.90%, N, 9.83%. Found: C, 59.06%; H, 5.88%, N, 9.83%.

4-(4-(4-Fluoro-3-(trifluoromethyl)phenyl)-1-methyl-1*H*-imidazol-2-yl)piperidine (5). An anhydrous HCl solution was prepared by slow addition of acetyl chloride (16.2 kg, 206.4 mol, 4.00 equiv) to methanol (88 L) over 45 min at <5 °C. The resulting solution was then added to a separate flask containing a solution of **3** (22 kg, 51.5 mol) in methanol (88 L) over 90 min at 20 °C, rinsing forward with MeOH (12 L). The reaction mixture was stirred at 20 °C for 14 h at which point HPLC analysis showed no **3** remaining. Dimethyl sulfoxide (115 L) was then added, and the reaction mixture was then concentrated under vacuum (150 mmHg at 30 °C) to a total volume of 110 L. Dimethyl sulfoxide (29 L) was then added back to the tank in one portion, and the distillation resumed. DMSO (84 L) was then added continuously to the tank during the distillation to maintain a constant volume of 139 L. The pressure was maintained at 20 mmHg. The temperature of the solution gradually increased from 5 to 6 °C at the beginning of distillation to 50−55 °C by the end of distillation. Dimethyl sulfoxide (125 L) was then added, and the solution was cooled to 20 °C. At this point the reaction mixture should contain <500 ppm MeOH. Triethylamine (21.7 kg, 214 mol, 4 equiv) is then added over 45 min at 15−25 °C to yield **5** as a solution in DMSO for use in subsequent chemistry. Compound **5** was also crystallized and fully characterized. For these data see the kilogram run in the PFR later in the Experimental Section.

***tert*-Butyl Methyl(2-morpholino-2-oxoethyl)carbamate (21).** To a 22 L three-neck round-bottom flask (RBC) equipped with N_2 sweep was added **20** (1500 g, 7.93 mol) and ethyl acetate (15 L). 1,1′-Carbonyldiimidazole (CDI) (1542 g, 9.52 mol) was added as a solid to the mixture over 10 min at room temperature. The reaction mixture was stirred at room temperature for 3−4 h. Morpholine (829 g, 9.52 mol) was then added, and the reaction mixture was stirred at room temperature for an additional 16 h. Water (7.5 L) was added to the reaction mixture, and the layers were separated. The aqueous layer was extracted with ethyl acetate (2 × 7.5 L). The combined organic layers were washed with 1 N HCl (7.5 L), followed by water (7.5 L), and then were dried over 700 g of Na_2SO_4. The solution was filtered, and the filtrate was concentrated under reduced pressure at 50−55 °C to afford **21** (1370 g, 5.3 mol, 67% yield) as a yellow oil. The crude mixture was used in the next step without further purification. ^{1}H NMR ($CHCl_3$) δ 4.03 (s, 2 H), 3.65 (s, 4 H), 3.59 (d, 2 H, J = 3.2 Hz), 3.43 (s, 2 H), 2.91 (s, 3 H), 1.43 (d, 9 H, J = 14.0 Hz); ^{13}C NMR ($CHCl_3$) δ 80.1, 66.8, 66.5, 50.0, 45.2, 42.1, 35.4, 28.3; IR ($CHCl_3$) 2973, 2857, 1696, 1663, 1456, 1177, 1115, 1032, 772 cm^{-1}; Exact Mass: Calcd m/z for $C_{12}H_{23}N_2O_4^+$: 259.1652, Found: 259.1649.

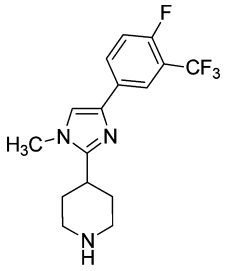

5

1-(4-Fluoro-3-(trifluoromethyl)phenyl)-2-(methylamino)-ethanone Hydrochloride (24). To a 2 L three-neck RBF equipped with N_2 sweep was charged 4-bromo-1-fluoro-2-(trifluoromethyl)benzene (103.3 g, 425 mmol) and THF (175 mL). The reaction mixture was purged with N_2 twice. Isopropyl magnesium chloride (2 M solution in THF, 203 mL,

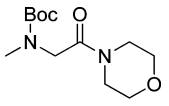

21

406 mmol) was added dropwise over 20 min at room temperature. The reaction mixture was then stirred at room temperature for 2−3 h resulting in **22**. A solution of **21** (50 g, 194 mmol) in THF (50 mL) was added dropwise over 10 min at 25−45 °C. The reaction mixture was stirred at room temperature for 5 h. The reaction was then quenched with saturated NH_4Cl solution (50 mL). Ethyl acetate (600 mL) was added, followed by water (250 mL). The pH of the aqueous layer was adjusted to 5−7 with 1 N HCl. Upon acidification, clear layer separation was observed. The layers were separated, and the aqueous layer was extracted with ethyl acetate (200 mL). The combined organic layer was washed with brine (250 mL) and dried with Na_2SO_4 (100 g). The organic layer was then filtered, and the filtrate was concentrated under reduced pressure to afford **23** (70.9 g, 211.5 mmol,

dx.doi.org/10.1021/op200351g | *Org. Process Res. Dev.* 2012, 16, 982−1002

109% recovery) as a dark-brown oil, which was used in the next step without further purification. To a three-neck (RBF) equipped with N_2 sweep was charged **23** (70.9 g, 211.5 mmol) and ethyl acetate (35 mL). The reaction mixture was cooled to 0−10 °C using an ice bath. HCl (2.0 M solution in ethyl acetate, 994.1 mmol) was added dropwise at a rate sufficient to maintain the temperature at 0−10 °C. The reaction mixture was then stirred under N_2 at room temperature for 16−20 h. The reaction mixture was filtered, and the cake was rinsed with 0−10 °C ethyl

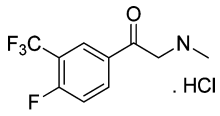

24

acetate (70 mL). The wet cake was slurried with ethyl acetate (35 mL) at room temperature, and the mixture was filtered. The cake was dried under vacuum at 40−50 °C to afford **24** (56.4 g, 208.3 mmol, 49% yield from **21**) as a white solid. ^{1}H NMR (DMSO-d_6) δ 9.48 (s, 2 H), 8.36 (m, 2 H), 7.77 (t, 1 H, J = 10.0 Hz), 4.82 (s, 2 H), 2.59 (s, 3 H); ^{13}C NMR (DMSO-d_6) δ 91.0, 136.2, 136.1, 131.1, 131.1, 128.3, 121.2, 118.9, 118.7, 54.0, 33.1; IR (KBr mull cm^{-1}) 2922, 2781, 2703, 1687, 1333, 1278, 1146, 1053, 848 cm^{-1}; Exact Mass: Calcd m/z for $C_{10}H_{10}ONF_4$: 236.0693, Found: 236.0221. See Supporting Information for HPLC chromatogram.

***tert*-Butyl 4-((2-(4-Fluoro-3-(trifluoromethyl)phenyl)-2-oxoethyl)(methyl)carbamoyl)piperidine-1-carboxylate (6).** To a 3 L three-neck RBF was added **24** (800 g, 2.95 mol), 1-(*tert*-butoxycarbonyl)piperidine-4-carboxylic acid (743 g, 3.24 mol), and THF (8.0 L). The reaction mixture was cooled to 0−5 °C using an ice−water bath. 1-Propanephosphonic acid cyclic anhydride (T_3P, 50% wt. solution in ethyl acetate, 3186 g, 5.02 mol) was added dropwise at a rate sufficient to maintain an internal temperature of 0−5 °C. Finally, *N*-methylmorpholine (3186 g, 11.56 mol) was added dropwise at a rate sufficient to maintain an internal temperature of 0−5 °C. Upon *N*-methylmorpholine addition, the reaction mixture became a solution. The reaction mixture was warmed to room temperature and was stirred for 20 h. Ethyl acetate (6.4 L) was added, followed by water (6.4 L). The layers were separated. The aqueous layer was extracted with ethyl acetate (3.2 L). The combined organic layer was washed with brine (3.2 L) and dried over Na_2SO_4. The mixture was then filtered, and the filtrate was concentrated under reduced pressure to afford crude **6** as a dark oil. Ethyl acetate (2000 mL) was added to the dark oil, and a solution was formed. Heptane (7000 mL) was added to the solution dropwise, and a slurry was observed. The resulting slurry was stirred at room temperature for 3 h. The mixture was then filtered, and the cake was dried under reduced pressure at 40−50 °C to afford **6** (850 g, 1.90 mol, 65% yield) as a white solid. ^{1}H NMR ($CHCl_3$) δ 8.8.22 (d, 1 H, J = 6.8 Hz), 8.16 (m, 1 H), 4.76 (s, 2 H), 4.13 (m, 2 H), 3.17 (s, 3 H), 2.77 (m, 2 H), 1.72 (m, 4 H), 1.44 (s, 9 H); ^{13}C NMR ($CHCl_3$) δ 192.1, 175.2, 154.7, 134.0, 133.9, 131.5, 131.4,

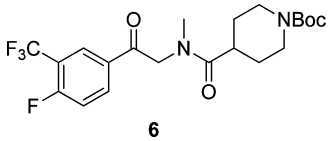

6

127.7, 127.7, 117.7, 117.5, 79.6, 54.3, 38.5, 36.6, 28.4, 28.0; IR (KBr mull) 2981, 2926, 1633, 1505, 1366, 1281, 1215, 1140, 1056 cm^{-1}; Exact Mass: Calcd m/z for $C_{21}H_{26}F_4N_2O_4Na^+$: 469.1721, Found: 469.1712. See Supporting Information for HPLC chromatogram.

***tert*-Butyl 4-(4-(4-Fluoro-3-(trifluoromethyl)phenyl)-1-methyl-1*H*-imidazol-2-yl)piperidine-1-carboxylate (7).** A solution of **6** 1232.14 g (2.7599 mol) and acetic acid (3314 g, 55.2 mol) in methanol (3080 mL) was prepared. A solution of ammonium acetate (2162 g, 8.94 equiv, 28.05 mol) and methanol (5600 mL) was prepared separately.

Separate high-pressure syringe pumps were used to flow the two solutions. The solutions mixed at a standard T-shaped fitting and then immediately flowed through a stainless steel coiled tube reactor (221 mL reactor listed in Table 10) which had been pressurized to 1000 psig with nitrogen and heated in an oil bath to 140 °C. Flow rates were controlled such that the molar ratio of ammonium acetate was 10:1 with respect to **6** and $V_{reactor}/Q_{feed}$ = 10 min at which point the solution cooled to ambient temperature in a tube-in-tube heat exchanger and exited the system via the back-pressure regulator to be collected. HPLC samples were pulled via an automated sampling and dilution system every 10 min throughout the course of the 20 h run. Typical steady-state composition by HPLC was **16** (3.7%), **1** (0.2%), **17** (0.1%), and **2** (95.5%). HPLC conditions: Zorbax SB Phenyl 4.6 mm × 50 mm, 1.8 μm; 1.0 mL/min, 40 °C; 260 nm Solvent A: 0.2% (w/v) NH_4OAc in H_2O, Solvent B: 0.1% (v/v) AcOH in ACN; Gradient: 0 min (80% A/20% B); 10 min (20% A/80% B); 11 min (20% A/80% B); 11.1 min (80% A/20% B).

The product solution was divided equally between identical 22 L flasks (6640 g in each), and the following procedure was followed on each flask to crystallize. The clear, orange solution was heated to 50 °C under nitrogen. Water (6 L) was added dropwise at 50 °C. After 2000 mL had been added, the solution was seeded and the product precipitated. After 6 L was added, the tan slurry was heated at 50 °C for 1 h; then the heat was turned off, and the slurry was allowed to cool to room temperature in the heating mantle overnight. The total amount of water used to crystallize all of the product in both flasks was 12 L. The product was filtered and the cake washed with 1:1 MeOH/water (3 L). The solids were dried in a vacuum oven at 50 °C to afford **7**, 1009.5 g (75.3% yield). See earlier experimental for characterization data.

4-(4-(4-Fluoro-3-(trifluoromethyl)phenyl)-1-methyl-1*H*-imidazol-2-yl)piperidine (5). A solution of **7** (1000 g, 2.34 mol) in a mixture of tetrahydrofuran (20 L) and methanol (1 L) was flowed through a stainless steel coiled tube reactor (221 mL reactor listed in Table 10) which had been pressurized to 1000 psig with nitrogen and heated in a standard GC oven to 270 °C. The flow rate were controlled such that $V_{reactor}/Q_{feed}$ = 15 min at which point the solution cooled to ambient temperature in a tube-in-tube heat exchanger and exited the system via the back-pressure regulator to be collected. The total collected reaction mixture was concentrated to a solid (771 g, 97% yield, potency corrected). 717 g of this solid was dissolved in toluene (4.8 L) in a 22 L RBF at 50 °C. Heptane (7 L) was added slowly via add'n funnel. After 1 L had been added the solution was seeded and thin slurry developed. The remaining heptane was added over ∼1 h and the slurry stirred at 50 °C for 20 min, then allowed to cool to room temperature overnight in a heating mantle. Solids were filtered, and the cake was washed with 1 L of 10% toluene in heptane. Solids were dried in a vacuum oven at 50 °C overnight to afford **5** (573.6 g, 80% recovery) as a white solid (mp 147−150 °C). ^{1}H NMR (400 MHz, DMSO) δ

dx.doi.org/10.1021/op200351g | Org. Process Res. Dev. 2012, 16, 982−1002

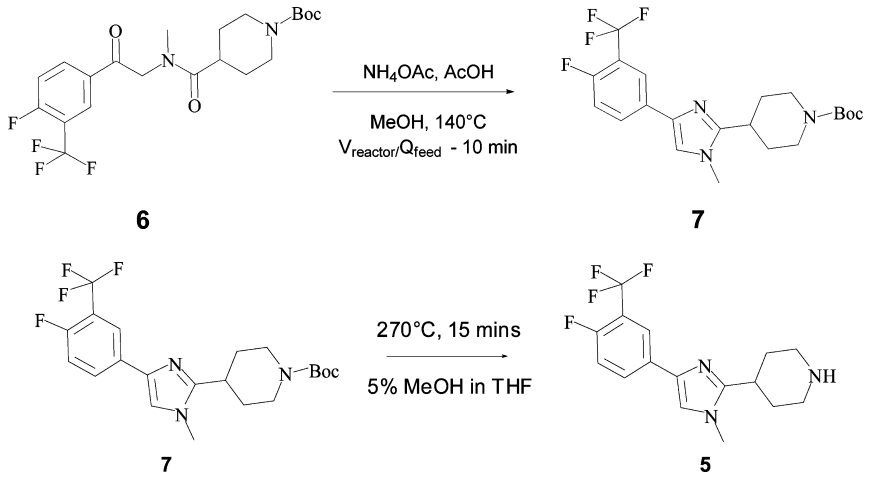

7.99–7.96 (m, 2H), 7.60 (s, 1H), 7.42 (t, J = 9.9 Hz, 1H), 3.58 (s, 3H), 2.97 (d, J = 12.3 Hz, 2H), 2.83–2.76 (m, 1H), 2.54 (td, J = 11.9, 2.1 Hz, 2H), 1.70–1.57 (m, 4H); ^{19}F NMR (376.2 MHz, DMSO-d_6) δ −61.48 (d, J = 13.29 Hz, 3F), −111.84 (m, 1F); IR (neat solid, ν/cm^{-1}) 3304.4, 2939.8, 2805.8, 1555.5, 1495.9, 1458.7, 1436.4, 1324.8, 1295.0. 1228.0, 1198.2, 1116.4, 1049.4, 960.1. 893.1, 833.6, 788.9, 759.1; HRMS (ESI): predicted for $C_{16}H_{18}F_4N_3^+$: 328.1423, found 328.1431. See Supporting Information for HPLC chromatogram.

■ ASSOCIATED CONTENT

Supporting Information

Select HPLC data as an additional demonstration of purity for compounds **11a**, **13**, **24**, **6**, and **5**. This material is available free of charge via the Internet at http://pubs.acs.org.

■ AUTHOR INFORMATION

Corresponding Author

*E-mail: (S.A.M.) May_Scott_A@Lilly.com; (J.D.M.) Johnson_Martin_D@Lilly.com.

Present Address

‡D&M Continuous Solutions, 7814 Pennyroyal Lane, Indianapolis, IN, 46237.

Notes

The authors declare no competing financial interest.

▼Deceased December 26, 2007.

■ ACKNOWLEDGMENTS

We thank Paul Milenbaugh and Ed H. Deweese of D&M Continuous Solutions (Greenwood, IN) for assembly and operation of most of the PFR systems in this paper. We thank the reviewer who recommended improvements to the axial dispersion sections of this paper. We thank Adam McFarland and Randy Lambertus for on-line Raman probe measurements used to characterize the tube reactors for axial dispersion. We also thank Zheng Chen, John P. Schafer, and John Howell for select work on the alkylation of compound **2** and scale up shown in Table 1. We also acknowledge Asymchem for the pilot-scale preparation of ketoamide **1**. Finally we thank Bret Huff for his vision and support in continuous processing at Lilly.

■ REFERENCES

(1) Alvarez-Builla, J., Vaquero, J. J, Barluenga, J., Eds. *Modern Heterocyclic Chemistry*; 2011; Vol. *2*

(2) Katritzky, A. R., Ramsden, C. A., Joule, J. A., Zhdankin, V. V., Eds. *Handbook of Heterocyclic Chemistry*, 3rd ed.; Oxford: New York, 2011; Vol. *133*.

(3) Chen, S.-B.; Tan, J.-H.; Ou, T.-M.; Huang, S.-L.; An, L.-K.; Luo, H.-B.; Li, D.; Gu, L.-Q.; Huang, Z.-S. *Bioorg. Med. Chem. Lett.* **2011**, *21*, 1004.

(4) Zotova, S.; Shvedov, V. *Pharm. Chem. J.* **1994**, *28*, 103.

(5) Revuelta, J.; Machetti, F.; Cicchi, S. *Mod. Heterocycl. Chem.* **2011**, *2*, 809.

(6) Weintraub, P. M.; Meyer, D. R.; Aiman, C. E. *J. Org. Chem.* **1980**, *45*, 4989.

(7) It is also interesting to note that resin-bound azide performed very well in alcoholic solvents as a safer alternative to using solid sodium azide. Unfortunately, this azide source did not work as well in THF, which was required to telescope the steps.

(8) Gupton, J. T.; Miller, R. B.; Krumpe, K. E.; Clough, S. C.; Banner, E. J.; Kanters, R. P. F; Du, K. X.; Keertikar, K. M.; Lauerman, N. E.; Solano, J. M.; Adams, B. R.; Callahan, D. W.; Little, B. A.; Scharf, A. B.; Sikorski, J. A. *Tetrahedron* **2005**, *61*, 1845.

(9) This generates very little pressure in the vessel, but the sealed system prevents ammonia loss and allows for full conversion without recharging ammonium acetate.

(10) As measured from solvent-only runs.

(11) This results in feed rates of 0.011 mL/min of a 0.2442 M solution of ketoamide feed and 0.028 mL/min of a 0.0964 M solution of TEA/NH_4OAc.

(12) For safety, simplicity, and cost reasons, forced convection ovens are used in place of oil baths for temperatures >140 °C.

(13) Full details of this equipment set are available in the Experimental Section.

(14) Reaction composition for this temperature screen was 17 vol equiv of methanol, 1 equiv of triethylamine, and 10 equiv of ammonium acetate.

(15) Since mean residence time was not known for each of the temperatures in the screen, these data could not be used for understanding the reaction kinetics. This would be important if one wanted to apply data to other reactor dimensions or types such as stirred tanks.

(16) We determined that triethylamine was not necessary prior to the stoichiometry optimization.

(17) This is with a relatively long reaction without any integrated PAT to aid in sample collection and analysis.

(18) Decreasing d to 0.254 mm, a standard size for stainless steel tubing, would further reduce the material requirement. This has been necessary when dealing with new route scouting where material is not abundantly available. Usually, however, the material availability is sufficient for using tube reactors with d = 0.56 mm which is less prone to clogging.

(19) One equivalent of triethylamine was present in the 20-g scale-up. It was later found that TEA had no effect on the outcome of the reaction and TEA was not used in the 775-g-scale reaction.

(20) Other oligomeric impurities were present, but **18** was specifically identified in HPLC traces. **18** can also undergo further reaction to deliver numerous oligomeric impurities.
(21) While no significant pressure builds because the 1-butanol boiling point is 118 °C, the loss of ammonia is an issue in normal glassware. Running this type of reaction require recharging of ammonium acetate to drive the reaction to completion.
(22) Five equivalents of NH_4OAc at $V_{reactor}/Q_{feed}$ = 90 min.
(23) Since we did not observe product degradation, even at elevated temperatures and for long residence times, we concluded that the degration of the ketoamide was the primary issue.
(24) Levenspiel, O. *Chemical Reaction Engineering. An Introduction to the Design of Chemical Reactors*; John Wiley and Sons, Inc.: New York, NY, 1962.
(25) A second campaign was later conducted where the reaction, workup, and isolation were all conducted continuously. This was beyond the scope of this paper and will be reported in due course.
(26) Grignard reagent was made through exchange between isopropylmagnesium chloride and 4-fluoro-3-trifluoromethyl-1-bromobenzene in THF at RT.
(27) The first experiments showing this result were conducted in acetic acid as the solvent with a large excess of ammonium acetate.
(28) Klint, D.; Bovin, J.-O. *Mater. Res. Bull.* **1999**, *34*, 721.
(29) Reik, R. *Monatsh. Chem.* **1902**, *23*, 1033.
(30) Ammonium acetate has a solubility of 45.9 mg/mL in methanol and 16.3 mg/mL in ethanol.
(31) One notable result from this screen, however, is the finding that an 86% in situ yield can be obtained after just one minute residence time at 180 °C, even in the presence of 20 equiv of AcOH. This represents a 1200× rate acceleration vs the batch reaction conditions at only slightly lower yield.
(32) In the 7 L PFR described in this paper, 44.8 kg of **6** could be produced in a day. Increasing the reactor to 73 L described elsewhere by us would afford 467 kg/day throughput.
(33) The yield on 1 kg scale was lower than expected and likely due to potency issues with the batch of **1** used. Reactions in smaller reactors were higher, and there is no reason to expect a yield difference between reactors.
(34) τ was measured in a separate flow experiment using product only in the reaction solvent.
(35) Not shown because the F-curves for the 221 mL PFR look practically identical to those for the 4.51 mL PFR.
(36) Global FIA, 684 Sixth Ave. FI, Fox Island, WA 98333, United States.
(37) It is important to have safety precautions in place for any unattended operation. Pressure relief for the reactor and pumps and automatic shutoffs on the pumps are essential in the event the system becomes clogged and overpressurizes.
(38) (a) Levenspiel, O. *The Chemical Reactor Omnibook*; Oregon State University Book Stores, Inc.: Corvallis, OR, 1993. (b) Levenspiel, O. *Chemical Reaction Engineering. An Introduction to the Design of Chemical Reactors*; John Wiley and Sons, Inc.: New York, NY, 1962. (c) Fogler, H. S. *Elements of Chemical Reaction Engineering*, 3rd ed.; Prentice Hall PTR: Upper Saddle River, NJ, 1999. (d) Walter, J., Weber, J., DiGiano, F. A., Eds. *Process Dynamics in Environmental Systems*; John Wiley and Sons, Inc.: New York, NY, 1996. (e) Aris, R. On the Dispersion of a Solute in a Fluid Flowing through a Tube. *Proc. R. Soc. Lond., Ser. A* **1956**, *235*, 67–77. (f) Taylor, G. Dispersion of Soluble Matter in a Solvent Flowing Slowly through a Tube. *Proc. R. Soc. Lond., Ser. A* **1953**, *219*, 186–203. (g) Taylor, G. Dispersion of Matter in Turbulent Flow through a Pipe. *Proc. R. Soc. Lond., Ser. A* **1954**, *223*, 446–468. (h) Taylor, G. Conditions under which dispersion of a solute in a stream of solvent can be used to measure molecular diffusion. *Proc. R. Soc. Lond., Ser. A* **1954**, *223*, 473–477.
(39) Levenspiel, O. Chemical Reaction Engineering. In *An Introduction to the Design of Chemical Reactors*; John Wiley and Sons, Inc.: New York, NY, 1962.
(40) Dankwerts, P. V. *Ind. Chemist* **1954**, *3*, 102.
(41) Levenspiel, O. Longitudinal Mixing of Fluids Flowing in Circular Pipes. *Ind. Eng. Chem.* **1958**, *50*, 343–346.
(42) Levenspiel, O. *The Chemical Reactor Omnibook*; Oregon State University Book Stores, Inc.: Corvallis, OR, 1993.
(43) Table 10 can serve as a guideline for selecting an appropriate reactor.
(44) Hickman, D. A.; Sobeck, D. D.; In Liquid Phase Process Characterization. *Micro Instrumentation: for High Throughput Experimentation and Process Intensification - A Tool for PAT*; Koch, M. V., VandenBussche, K. M., Chrisman, R. W., Eds.Wiley, New York, NY, 2007; Chapter 13.
(45) Green, D. W.; Perry, R. H. *Perry's Chemical Engineers' Handbook*.8th ed. McGraw-Hill: New York, 2008.
(46) Bromide, **7a**, is also commercially available, but due to project timelines, we chose to make it in this case.
(47) Typically <7% acetophenone, ~8% bis-Br, ~84% **7a**.
(48) Despatch Industries, LND1-42-3, Inert Atmosphere Oven for use in Class I, Division 2 Area.

NOTE ADDED AFTER ASAP PUBLICATION

This paper was published on the Web on April 19, 2012. Figure 13 has been updated and the corrected version was reposted on April 26, 2012.